

Semismooth Newton Coordinate Descent Algorithm for Elastic-Net Penalized Huber Loss and Quantile Regression

Congrui Yi and Jian Huang

Department of Statistics and Actuarial Science
University of Iowa
Iowa City, IA 52242
U.S.A.

Abstract

We propose a semismooth Newton coordinate descent (SNCD) algorithm for elastic-net penalized robust regression with Huber loss and quantile regression. The SNCD is a novel combination of the semismooth Newton and coordinate descent algorithms. It is designed for loss functions with only first order derivatives and is scalable to high-dimensional models. Unlike the standard coordinate descent method, the SNCD updates the regression parameters and the corresponding subdifferentials based on the concept of Newton derivatives. In addition, an adaptive version of the “strong rule” for screening predictors is incorporated to gain extra efficiency. As an important application of the proposed algorithm, we show that the SNCD can be used to compute the solution paths for penalized quantile regression. We establish the convergence properties of the algorithm. Through numerical experiments, we demonstrate that the proposed algorithm works well for high-dimensional data with heavy-tailed errors, and that for quantile regression SNCD is considerably faster than the existing method and has better optimization performance. A breast cancer gene expression data set is used to illustrate the proposed algorithm.

Keywords: High-dimensional regression; Newton derivatives; Non-smooth optimization; Solution path; Subdifferential updating.

1 Introduction

Consider a linear regression model

$$y_i = \beta_0 + x_i^\top \beta + \varepsilon_i, i = 1, \dots, n,$$

where y_i is a response variable, x_i is a p -dimensional covariate, (β_0, β) are unknown parameters, and ε_i is an error term. We develop a fast and scalable algorithm to compute the solution paths for penalized Huber loss and quantile regression models, formulated as the convex optimization problem

$$\min_{\beta_0, \beta} \frac{1}{n} \sum_i \ell(y_i - \beta_0 - x_i^\top \beta) + \lambda P_\alpha(\beta), \quad (1.1)$$

where $\lambda \geq 0$ is a penalty parameter, ℓ is the Huber or quantile loss function, and $P_\alpha(\cdot)$ is the elastic-net penalty (Zou and Hastie, 2005)

$$P_\alpha(\beta) = \alpha \|\beta\|_1 + (1 - \alpha) \cdot \frac{1}{2} \|\beta\|_2^2,$$

which includes ℓ_1 (Tibshirani, 1996) and ℓ_2 penalties as special cases when $\alpha = 1$ and 0 , respectively. The Huber loss function is

$$\ell(t) \equiv h_\gamma(t) = \begin{cases} |t| - \frac{\gamma}{2} & \text{if } |t| > \gamma, \\ \frac{t^2}{2\gamma} & \text{if } |t| \leq \gamma. \end{cases} \quad (1.2)$$

This function is quadratic for small $|t|$ and linear when $|t|$ is greater than the threshold parameter γ . In addition, it is convex and first-order differentiable. These features allow us to combine analytical tractability of the squared loss used in least squares (LS) regression and robustness of the absolute loss in least absolute deviations (LAD) regression.

The quantile loss is

$$\ell(t) \equiv \rho_\tau(t) = t(\tau - I(t < 0)). \quad (1.3)$$

Rather than modeling the conditional mean of the response given the values of predictors, quantile regression models the conditional quantile of the response given the predictors. It includes the least absolute deviations (LAD) regression as a special case. This model has wide applications in statistics, econometrics and ecology, among others.

There is a large body of literature on these models in lower dimensional settings (Holland and Welsch, 1977; Huber, 1973; Huber, 1981; Koenker, 2005; Koenker and Bassett Jr, 1978). There has also been recent efforts in studying the theoretical properties of penalized high-dimensional robust regression, including the quantile regression. However, there is a lack of efficient algorithms and publicly available software for fitting penalized Huber loss and quantile regressions in high dimensional settings.

Recently, coordinate descent algorithms have proven to be useful and effective for pathwise optimization problems in high-dimensional regression models (Friedman et al., 2007; Friedman et al., 2010; Simon et al., 2011; Breheny and Huang, 2011). In all these examples, it is worth noting that either the loss function is quadratic for least squares regression with a simple closed-form solution for each iteration, or the loss function is the likelihood for generalized linear models that is at least twice differentiable and the Taylor expansion can be employed to form a local quadratic approximation, for which similar updates are again readily available. But the Huber loss is only first-order differentiable, hence the above approach does not apply. Although Wu and Lange (2008) considered a coordinate descent algorithm for LAD regression, there is no guarantee for the convergence of the algorithm in that paper.

An approach for dealing with nonsmooth optimization problems is the semismooth Newton algorithm (SNA) (Chen et al., 2000; Qi, 1993; Qi and Sun, 1993). It applies the concept of “Newton differentiability” to generate Newton-type iterations for solving nonsmooth equations. Reformulating the KKT conditions into a system of nonsmooth equations, we can obtain a convergent algorithm. However, despite theoretical superlinear convergence, the algorithm scales badly with the number of predictors p since number of arithmetic operations per iteration is $O(np^2)$.

In this paper, we propose a novel semismooth Newton coordinate descent (SNCD) algorithm for elastic-net penalized robust regression, including the Huber loss regression and quantile regression. This algorithm is designed for modeling high-dimensional data with nonsmooth loss functions. It is efficient and scalable for solving such high-dimensional problems. It is developed using a reformulated Karush-Kuhn-Tucker (KKT) condition based on the notion of proximity operator. Unlike the standard coordinate descent method which only updates the components of the parameter in the primal problem, the SNCD uses both the primal and dual information in the updating process. In addition, an adaptive version of the strong rule for screening predictors is incorporated to gain extra efficiency.

The SNCD combines the advantages of SNA and coordinate descent by applying SNA to solve each iteration of the latter. As a result, it is convergent and dramatically faster than SNA as the dimension increases. We also provide implementations of SNCD for penalized Huber loss regression and quantile regression through the publicly available R package `hqreg` (<https://cran.r-project.org/web/packages/hqreg/index.html>). In addition, we give examples with simulated and real data, demonstrating the efficiency of the proposed algorithm and its applications.

In section 2 we give an introduction to Newton differentiability and SNA. In particular SNA for elastic-net penalized Huber loss regression is derived and shown to converge superlinearly. In section 3, we present SNCD and its convergence guarantee. Then its applica-

tions to penalized Huber loss and quantile regression are discussed. In section 4, we describe an adaptive version of the strong rule (Tibshirani et al., 2012), a useful technique to discard predictors for computational efficiency. Then the connections between Huber loss, quantile, LS, and LAD regression are investigated in section 5, demonstrating the convergence of solutions of Huber loss regression to those of LS, LAD and quantile regression (plus an extra linear term) with the same penalty. In section 6 we compare `hqreg` and an existing R package `quantreg` (<https://cran.r-project.org/web/packages/quantreg/index.html>) for optimization on penalized quantile regression in different data scenarios, which indicates that `hqreg` has better performance. In section 7, a number of comparative timing experiments are given for both penalized Huber loss and quantile regression, noticeably showing that `hqreg` is considerably faster than `quantreg`. In Section 8, for a gene expression data set, we show that Huber loss performs better than the squared loss in the presence of heavy-tailed errors. Concluding remarks are given in Section 9.

2 Semismooth Newton Algorithm

2.1 Reformulation of KKT Conditions

Due to the convexity of the Huber loss and elastic net penalty, the Karush-Kuhn-Tucker (KKT) conditions are necessary and sufficient for the minimizer of (1.1). These conditions can be stated as

$$\begin{cases} -\frac{1}{n} \sum_i \dot{h}_\gamma(y_i - \beta_0 - x_i^\top \beta) = 0, \\ -\frac{1}{n} \sum_i \dot{h}_\gamma(y_i - \beta_0 - x_i^\top \beta) x_{ij} + \lambda \alpha s_j + \lambda(1 - \alpha) \beta_j = 0, \\ s_j \in \partial|\beta_j|, \quad j = 1, \dots, p, \end{cases} \quad (2.1)$$

where $\dot{h}_\gamma(\cdot)$ is the gradient of $h_\gamma(\cdot)$ that takes the form

$$\dot{h}_\gamma(t) = \begin{cases} \text{sign}(t) & \text{if } |t| > \gamma, \\ \frac{t}{\gamma} & \text{if } |t| \leq \gamma, \end{cases}$$

and $\partial|t|$ represents the set of the subgradients of the absolute value function at t , that is,

$$\partial|t| = \begin{cases} \{\text{sign}(t)\} & \text{if } t \neq 0, \\ [-1, 1] & \text{if } t = 0. \end{cases}$$

The last row in (2.1) can also be written in vector notation as

$$s \in \partial\|\beta\|_1, \quad (2.2)$$

where $\partial\|\beta\|_1 = (\partial|\beta_1|, \dots, \partial|\beta_p|)^\top$.

Minimizing (1.1) is equivalent to solving the KKT system (2.1). A main difficulty is how to deal with (2.2). We rewrite it using the soft-thresholding operator. This can be done as follows. In general, for convex optimization problems, the KKT conditions can be stated in terms of Fermat's rule (Rockafellar, 1970)

$$0 \in \partial f(z^*) \Leftrightarrow z^* = \arg \min_z f(z),$$

where f is a convex function. This holds because $0 \in \partial f(z^*)$ if and only if $f(z) - f(z^*) \geq 0^\top(z - z^*) = 0$ for every z , that is, $z^* = \arg \min_z f(z)$. A more general result (Combettes and Wajs, 2005) is

$$w \in \partial f(z) \Leftrightarrow z = \text{Prox}_f(z + w), \quad (2.3)$$

where Prox_f is the *proximity operator* for f defined as

$$\text{Prox}_f(z) := \arg \min_x \frac{1}{2} \|x - z\|_2^2 + f(x).$$

The second statement can be shown as follows. Applying Fermat's rule,

$$z = \text{Prox}_f(z + w) = \arg \min_x \frac{1}{2} \|x - z - w\|_2^2 + f(x),$$

if and only if there exists $s \in \partial f(x)$ such that

$$0 = (z - z - w) + s = -w + s,$$

that is,

$$w = s \in \partial f(x).$$

Since the proximity operator of $|\cdot|$ is given in closed form by the soft-thresholding operator with threshold 1, i.e.

$$\text{Prox}_{|\cdot|}(z) = S(z) = \text{sign}(z)(|z| - 1)_+,$$

it follows from (2.3) that $s_j \in \partial|\beta_j|$ can be expressed as an equation

$$\beta_j - S(\beta_j + s_j) = 0.$$

More generally, the proximity operator for the ℓ_1 norm of a vector $z = (z_1, \dots, z_p)^\top$ is $\text{Prox}_{\|\cdot\|_1}(z) = \mathcal{S}(z) = (S(z_1), \dots, S(z_p))$. This implies

$$s \in \partial\|\beta\|_1 \Leftrightarrow \beta - \mathcal{S}(\beta + s) = 0.$$

Therefore, the KKT conditions (2.1) for the global optimization problem can be fully expressed as a system of equations. Define

$$d = d(\beta_0, \beta; \gamma) = \begin{bmatrix} \dot{h}_\gamma(y_1 - \beta_0 - x_1^\top \beta) \\ \vdots \\ \dot{h}_\gamma(y_n - \beta_0 - x_n^\top \beta) \end{bmatrix}. \quad (2.4)$$

the KKT conditions are

$$\begin{cases} -\frac{1}{n} \mathbf{1}^\top d = 0 \\ -\frac{1}{n} X^\top d + \lambda \alpha s + \lambda(1 - \alpha) \beta = 0 \\ \beta - \mathcal{S}(\beta + s) = 0. \end{cases}$$

So the optimizer of problem (1.1) can be found by solving this system of nonsmooth equations. This can be done by using the Semismooth Newton Algorithm.

2.2 Newton Differentiability and General SNA

Qi (1993) established superlinear convergence of a Newton-type method via a concept of “semismoothness” originally introduced by Mifflin (1977), hence the name Semismooth Newton Algorithm (SNA). Chen et al. (2000) introduced the concept of slanting or Newton differentiability, which captures a property that appears in establishing convergence of Newton-type methods for solving nonsmooth equations. Superlinear convergence is established based on the Newton differentiability, which is a weaker condition than that required in the original convergence results of Qi (1993). Therefore, we choose the latter one for our problem.

Definition 2.1. A function $F : \mathbb{R}^m \rightarrow \mathbb{R}^l$ is said to be *Newton differentiable* at $z \in \mathbb{R}^m$ if there exists an open neighborhood $\mathcal{N}(z)$ and a mapping $H : \mathcal{N}(z) \rightarrow \mathbb{R}^{l \times m}$ such that $\{H(z + h) : z + h \in \mathcal{N}(z), h \neq 0\}$ is uniformly bounded in spectral norm and

$$\|F(z + h) - F(z) - H(z + h)h\|_2 = o(\|h\|_2) \quad \text{as } h \rightarrow 0.$$

H is called a *Newton derivative* for F at z . The set of all Newton derivatives is denoted as $\nabla_N F(z)$.

Remarks.

- (1) Unlike other notions of differentiability, “ $H(z)$ ” does not appear in the above definition, so in general, for a Newton derivative H for F at z , $H(z)$ is not characterized by a limit of quotients. Actually, it can take any value.

(2) The requirement that H is uniformly bounded in the neighborhood of z is very important. Otherwise, any function F is Newton differentiable at z with $H(z+h) = (F(z+h) - F(z))h^\top/\|h\|_2^2$ as a Newton derivative.

Next, we list two results from Chen et al. (2000) and one from Ito and Kunisch (2008). The first one establishes superlinear convergence of SNA. The second shows Newton differentiability is equivalent to local Lipschitz continuity. And the third gives conditions for Newton differentiability on composite functions.

Theorem 2.1. *Suppose that $F : \mathbb{R}^m \rightarrow \mathbb{R}^m$ is Newton differentiable at a solution z^* of $F(z) = 0$. Let H be a Newton derivative for F at z^* . Suppose there exists a neighborhood $\mathcal{N}(z^*)$ and $M > 0$ such that $H(z)$ is nonsingular and $\|H(z)^{-1}\| \leq M$ for all $z \in \mathcal{N}(z^*)$, then the Newton-type iteration*

$$z^{k+1} = z^k - H(z^k)^{-1}F(z^k)$$

converges superlinearly to z^ provided that $\|z^0 - z^*\|_2$ is sufficiently small.*

Definition 2.2. A function $F : \mathbb{R}^m \rightarrow \mathbb{R}^l$ is said to be *Lipschitz continuous* at z if there exists $L > 0$ such that for all sufficiently small h ,

$$\|F(z+h) - F(z)\|_2 \leq L\|h\|_2.$$

Theorem 2.2. *A function $F : \mathbb{R}^m \rightarrow \mathbb{R}^l$ is Newton differentiable at z if and only if F is Lipschitz continuous at z .*

Lemma 2.3. *If $F : \mathbb{R}^l \rightarrow \mathbb{R}^m$ is continuously Fréchet differentiable at $z \in \mathbb{R}^l$ with Jacobian J_F and $G : \mathbb{R}^m \rightarrow \mathbb{R}^n$ is Newton differentiable at $F(z)$ with a Newton derivative H_G . Then $G \circ F$ is Newton differentiable at z with a Newton derivative $H_G(F(z+h))J_F(z+h)$ for h sufficiently small.*

In addition to this lemma, we derived some other results useful in constructing Newton derivatives.

Lemma 2.4. *In the following, assume $F : \mathbb{R}^m \rightarrow \mathbb{R}^l$, $G : \mathbb{R}^m \rightarrow \mathbb{R}^l$, $z \in \mathbb{R}^m$, $F = (F_1, \dots, F_l)^\top$ and $H = (H_1^\top, \dots, H_l^\top)^\top$, where $H_i \in \mathbb{R}^{1 \times m}$, $i = 1, \dots, l$.*

- (i) *If F is continuously Fréchet differentiable at z , then F is also Newton differentiable at z and $J_F \in \nabla_N F(z)$;*
- (ii) *If F is Newton differentiable at z , then for any integer $k > 0$ and $A \in \mathbb{R}^{k \times l}$, AF is Newton differentiable at z ; if $H \in \nabla_N F(z)$, then $AH \in \nabla_N AF(z)$;*

(iii) If F and G are Newton differentiable at z , then $F + G$ is Newton differentiable at z ;
if $H_F \in \nabla_N F(z)$, $H_G \in \nabla_N G(z)$, then $H_F + H_G \in \nabla_N(F + G)(z)$;

(iv) F is Newton differentiable at z if and only if F_1, \dots, F_l are all Newton differentiable at z and $H \in \nabla_N F(z) \Leftrightarrow H_i \in \nabla_N F_i(z)$, $i = 1, \dots, l$;

Lemma 2.5. A univariate piecewise-smooth real function f is everywhere Newton differentiable, with a Newton derivative H given by

$$H(z) = \begin{cases} f'(z) & \text{if } f \text{ is differentiable at } z, \\ r_z \in \mathbb{R}^1 & \text{if } f \text{ is not differentiable at } z. \end{cases}$$

2.3 SNA for Penalized Huber Loss Regression

Let

$$Z = \begin{bmatrix} s \\ \beta_0 \\ \beta \end{bmatrix} \quad \text{and} \quad F(Z) = \begin{bmatrix} F_1(Z) \\ F_2(Z) \\ F_3(Z) \end{bmatrix},$$

where

$$\begin{aligned} F_1(Z) &= \beta - \mathcal{S}(\beta + s), \\ F_2(Z) &= -\frac{1}{n} \mathbf{1}^\top d(\beta_0, \beta; \gamma), \\ F_3(Z) &= -\frac{1}{n} \mathbf{X}^\top d(\beta_0, \beta; \gamma) + \lambda \alpha s + \lambda(1 - \alpha)\beta. \end{aligned}$$

Note that $\mathcal{S}(\beta + s) = (S(\beta_1 + s_1), \dots, S(\beta_p + s_p))^\top$ and S is a soft-thresholding operator defined by

$$S(t) = \text{sign}(t)(|t| - 1)_+ = \begin{cases} t - \text{sign}(t) & \text{if } |t| > 1, \\ 0 & \text{if } |t| \leq 1. \end{cases} \quad (2.5)$$

This motivates us to define

$$\begin{aligned} A &= A(Z) = \{j : |\beta_j + s_j| > 1\}, \\ B &= B(Z) = \{j : |\beta_j + s_j| \leq 1\}. \end{aligned} \quad (2.6)$$

The set A works as an estimate for the support of β . In fact, if $\hat{Z} = (\hat{s}, \hat{\beta}_0, \hat{\beta})$ solves $F(Z) = 0$, then $A(\hat{Z})$ is exactly the support for $\hat{\beta}$. This is easy to see: since $\hat{s}_j \in \partial|\hat{\beta}_j|$, if $\hat{\beta}_j \neq 0$ then $|\hat{\beta}_j + \hat{s}_j| = |\hat{\beta}_j + \text{sign}(\hat{\beta}_j)| = |\hat{\beta}_j| + 1 > 1$, otherwise $|\hat{\beta}_j + \hat{s}_j| = |\hat{s}_j| \leq 1$. As shown later, this technique helps reduce dimension and gives rise to a feasible algorithm.

Continuing with the derivation, reorder Z and $F(Z)$ such that

$$Z = \begin{bmatrix} s_A \\ \beta_B \\ \beta_0 \\ \beta_A \\ s_B \end{bmatrix}, \quad F(Z) = \begin{bmatrix} F_1(Z) \\ F_2(Z) \\ F_3(Z) \end{bmatrix} = \begin{bmatrix} \beta_A - \mathcal{S}(\beta_A + s_A) \\ \beta_B - \mathcal{S}(\beta_B + s_B) \\ -\frac{1}{n} \mathbf{1}^\top d \\ -\frac{1}{n} X_A^\top d + \lambda \alpha s_A + \lambda(1-\alpha)\beta_A \\ -\frac{1}{n} X_B^\top d + \lambda \alpha s_B + \lambda(1-\alpha)\beta_B \end{bmatrix}. \quad (2.7)$$

Then from (2.5) we have

$$F_1(Z) = \begin{bmatrix} -s_A + \text{sign}(\beta_A + s_A) \\ \beta_B \end{bmatrix}. \quad (2.8)$$

Now define

$$\psi_\gamma(t) = \frac{1}{\gamma} I(|t| \leq \gamma). \quad (2.9)$$

By Lemma 2.5, $\psi_\gamma \in \nabla_N \dot{h}(t)$ for any $t \in \mathbb{R}$. For simplicity, let $\psi_i(\beta_0, \beta) = \frac{1}{n} \psi_\gamma(y_i - \beta_0 - x_i^\top \beta)$, and $\Psi = \text{diag}(\psi_1, \dots, \psi_n)$. Then the following result gives a proper Newton derivative of F .

Theorem 2.6. $F(Z)$ is Newton differentiable for any $Z \in \mathbb{R}^{2p+1}$ and

$$H(Z) := \begin{bmatrix} -I_{|A|} & \mathbf{0} & 0 & \mathbf{0} & \mathbf{0} \\ \mathbf{0} & I_{|B|} & 0 & \mathbf{0} & \mathbf{0} \\ \mathbf{0} & \mathbf{1}_n^\top \Psi X_B & \mathbf{1}_n^\top \Psi \mathbf{1}_n & \mathbf{1}_n^\top \Psi X_A & \mathbf{0} \\ \lambda \alpha I_{|A|} & X_A^\top \Psi X_B & X_A^\top \Psi \mathbf{1}_n & X_A^\top \Psi X_A + \lambda(1-\alpha)I_{|A|} & \mathbf{0} \\ \mathbf{0} & X_B^\top \Psi X_B + \lambda(1-\alpha)I_{|B|} & X_B^\top \Psi \mathbf{1}_n & X_B^\top \Psi X_A & \lambda \alpha I_{|B|} \end{bmatrix} \in \nabla_N F(Z).$$

Furthermore, for any $\gamma > 0$ and $\alpha \in (0, 1)$, on the set $\{Z = (s, \beta_0, \beta) : \text{there exists } i \in \{1, \dots, n\} \text{ such that } |y_i - \beta_0 - x_i^\top \beta| \leq \gamma\}$, $H(Z)$ is invertible and $H(Z)^{-1}$ is uniformly bounded in spectral norm.

From Theorems 2.1 and 2.6, we immediately obtain the following result.

Theorem 2.7. Given $\lambda, \gamma, \alpha \in (0, 1)$, define Z and $F(Z)$ as (2.7). Suppose \hat{Z} solves $F(Z) = 0$ and there exists a neighborhood $\mathcal{N}(\hat{Z})$ such that for any $Z \in \mathcal{N}(\hat{Z})$ there is an $i \in \{1, \dots, n\}$ that satisfies $|y_i - \beta_0 - x_i^\top \beta| \leq \gamma$, then the Newton-type iteration

$$Z^{k+1} = Z^k - H(Z^k)^{-1} F(Z^k)$$

converges superlinearly to \hat{Z} provided that $\|Z^0 - \hat{Z}\|_2$ is sufficiently small.

Now we describe the algorithm in details. The $(k+1)$ -th iteration can be split into two steps:

1. Solve D_k from $H(Z^k)D_k = -F(Z^k)$;

2. Update $Z^{k+1} = Z^k + D^k$.

At first glance, step 1 seems to involve inverting a $(2p+1) \times (2p+1)$ matrix, which is infeasible in high dimensional settings. However, with the definitions of sets A, B in (2.6), sparsity of H_k can be utilized to reduce the dimension. Given the estimates from the k th iteration, define $d_k = d(\beta_0^k, \beta^k; \gamma)$, $A_k = A(Z^k)$, $B_k = B(Z^k)$ by (2.4) and (2.6) and reorder $Z^k, F(Z^k)$ as (2.7). Then correspondingly denote

$$D_k = \begin{bmatrix} D_{A_k}^s \\ D_{B_k}^\beta \\ D_0^{\beta_0} \\ D_{A_k}^\beta \\ D_{B_k}^s \end{bmatrix}. \quad (2.10)$$

Now substituting these identities into step 1 and combining (2.8) we have

$$\begin{aligned} D_{A_k}^s &= -s_{A_k}^k + \text{sign}(\beta_{A_k}^k + s_{A_k}^k), \\ D_{B_k}^\beta &= -\beta_{B_k}^k, \\ \begin{bmatrix} D_0^{\beta_0} \\ D_{A_k}^\beta \end{bmatrix} &= \begin{bmatrix} \mathbf{1}_n^\top \Psi_k \mathbf{1}_n & \mathbf{1}_n^\top \Psi_k X_{A_k} \\ X_{A_k}^\top \Psi_k \mathbf{1}_n & X_{A_k}^\top \Psi_k X_{A_k} + \lambda(1-\alpha)I_{|A_k|} \end{bmatrix}^{-1} \\ &\quad \begin{bmatrix} \frac{1}{n} \mathbf{1}^\top d_k + \mathbf{1}_n^\top \Psi_k X_{B_k} \beta_{B_k}^k \\ \frac{1}{n} X_{A_k}^\top d_k - \lambda(1-\alpha) \beta_{A_k}^k - \lambda \alpha \text{sign}(\beta_{A_k}^k + s_{A_k}^k) + X_{A_k}^\top \Psi_k X_{B_k} \beta_{B_k}^k \end{bmatrix}, \\ D_{B_k}^s &= -s_{B_k}^k + \frac{1}{\lambda \alpha} X_{B_k}^\top \left(\frac{1}{n} d_k + \Psi_k X_{B_k} \beta_{B_k}^k - \Psi_k \mathbf{1}_n D_0^{\beta_0} + \Psi_k X_{A_k} D_{A_k}^\beta \right). \end{aligned}$$

Combining steps 1 and 2, given the value at the k th iteration, the computation at the $(k+1)$ th iteration is carried out as follows:

(i) Update the subgradient s^{k+1} on A_k and set $\beta_{B_k}^{k+1}$ to zero:

$$\begin{aligned} s_{A_k}^{k+1} &= \text{sign}(\beta_{A_k}^k + s_{A_k}^k), \\ \beta_{B_k}^{k+1} &= \mathbf{0}. \end{aligned}$$

(ii) Update the search direction for $(\beta_0^{k+1}, \beta_{A_k}^{k+1})$:

$$\begin{bmatrix} D_0^{\beta_0} \\ D_{A_k}^{\beta} \end{bmatrix} = \begin{bmatrix} \mathbf{1}_n^\top \Psi_k \mathbf{1}_n & \mathbf{1}_n^\top \Psi_k X_{A_k} \\ X_{A_k}^\top \Psi_k \mathbf{1}_n & X_{A_k}^\top \Psi_k X_{A_k} + \lambda(1-\alpha)I_{|A_k|} \\ \frac{1}{n} \mathbf{1}^\top d_k + \mathbf{1}_n^\top \Psi_k X_{B_k} \beta_{B_k}^k \\ \frac{1}{n} X_{A_k}^\top d_k - \lambda(1-\alpha) \beta_{A_k}^k - \lambda \alpha s_{A_k}^{k+1} + X_{A_k}^\top \Psi_k X_{B_k} \beta_{B_k}^k \end{bmatrix}^{-1}.$$

(iii) Calculate the updated values of the intercept and coefficient on A_k , and the subgradient on B_k :

$$\begin{aligned} \beta_0^{k+1} &= \beta_0^k + D_0^{\beta_0}, \\ \beta_{A_k}^{k+1} &= \beta_{A_k}^k + D_{A_k}^{\beta}, \\ s_{B_k}^{k+1} &= \frac{1}{\lambda \alpha} X_{B_k}^\top \left(\frac{1}{n} d_k + \Psi_k X_{B_k} \beta_{B_k}^k - \Psi_k \mathbf{1}_n D_0^{\beta_0} + \Psi_k X_{A_k} D_{A_k}^{\beta} \right). \end{aligned}$$

2.4 Computational Bottleneck

Here we discuss the computational issues for the SNA described above. First, the algorithm requires inverting a positive definite matrix of dimension $(1 + |A_k|) \times (1 + |A_k|)$ at each iteration. In general, $|A_k|$ can be as large as p . But in our implementation of pathwise optimization, the algorithm is warm-started at each λ . That is, the coefficient vector computed at the previous λ is used as the initial value for the problem at current λ . In this situation, $|A_k|$ is usually $O(|S_0|)$ where S_0 denotes the support for the true coefficients. When the underlying true coefficients are sparse, matrix inversion is not the biggest issue.

The real bottleneck arises from the fact that the algorithm involves a lot of matrix multiplication at each iteration. Denoting augmented predictor matrix as $X^* = (\mathbf{1}_n \ X_{A_k} \ X_{B_k})$, then these computations altogether are essentially computing and subsetting $X^{*\top} \Psi_k X^*$, for which the number of arithmetic operations involved is at least of the order $O(np^2)$, which can be very large for big p . We have tried to optimize the implementation by utilizing the diagonality of Ψ_k and the symmetry of the resulting matrix, but these improvements could not reduce the order. Since $X^{*\top} \Psi_k X^* = \sum_i \psi_i(\beta_0^k, \beta^k) x_i^* x_i^{*\top}$, pre-storing all the $(1 + p) \times (1 + p)$ matrices $x_i^* x_i^{*\top}$ would speed up the computation, but since there are n such matrices, the implementation would make very poor use of cache memory.

3 Semismooth Newton Coordinate Descent

3.1 Description

SNA is a feasible approach for optimizing (1.1) for moderately large p , yet its efficiency is questionable due to large amount of matrix operations, which becomes problematic for

large p . For better efficiency and scalability, we propose a novel approach that combines the coordinate descent and SNA. In this approach, we solve the optimization problem under the coordinate descent framework, and apply SNA to solve the univariate subproblem in each iteration.

Consider the general elastic-net penalized regression model

$$\min_{\beta_0, \beta} f(\beta_0, \beta) = \frac{1}{n} \sum_i \ell(y_i - \beta_0 - x_i^\top \beta) + \lambda\alpha \|\beta\|_1 + \lambda(1-\alpha) \cdot \frac{1}{2} \|\beta\|_2^2, \quad (3.1)$$

where ℓ is coercive, convex and first-order (Fréchet) differentiable with derivative $\dot{\ell}$ and $\ddot{\ell}$ is Newton differentiable with $\ddot{\ell} \in \nabla_N \dot{\ell}(t), \forall t \in \mathbb{R}$. Since ℓ is convex, we can select $\ddot{\ell}$ such that $\ddot{\ell}(t) \geq 0$.

Denote the up-to-date coefficient estimates by $\tilde{Z} = (\tilde{\beta}_0, \tilde{\beta}, \tilde{s})$ and accordingly the current residuals $\tilde{r}_i = y_i - \tilde{\beta}_0 - x_i^\top \tilde{\beta}$. We proceed next by first providing a derivation of SNCD and then establishing its convergence.

Fixing λ and α , we find the optimizer $(\hat{\beta}_0, \hat{\beta})$ by minimizing the objective function with respect to one coefficient at a time:

(i) When updating β_0 , we keep all the coefficients fixed except β_0 , so the KKT conditions are

$$-\frac{1}{n} \sum_i \dot{\ell}(y_i - \beta_0 - x_i^\top \tilde{\beta}) = -\frac{1}{n} \sum_i \dot{\ell}(\tilde{r}_i + \tilde{\beta}_0 - \beta_0) = 0.$$

It can be shown that

$$\frac{1}{n} \sum_i \ddot{\ell}(\tilde{r}_i + \tilde{\beta}_0 - z) \in \nabla_N \left(-\frac{1}{n} \sum_i \dot{\ell}(\tilde{r}_i + \tilde{\beta}_0 - z) \right)$$

as a function of z . Hence we update β_0 via SNA as follows

$$\beta_0 \leftarrow \tilde{\beta}_0 + \frac{\sum_i \dot{\ell}(\tilde{r}_i)}{\sum_i \ddot{\ell}(\tilde{r}_i)}.$$

(ii) When updating $\beta_j, 1 \leq j \leq p$, we also update the corresponding subgradient s_j .

Similarly everything is fixed except β_j and s_j . The KKT conditions are

$$\begin{cases} -\frac{1}{n} \sum_i \dot{\ell}(\tilde{r}_i + x_{ij} \tilde{\beta}_j - x_{ij} \beta_j) x_{ij} + \lambda\alpha s_j + \lambda(1-\alpha) \beta_j = 0, \\ \beta_j - S(\beta_j + s_j) = 0. \end{cases} \quad (3.2)$$

Denote

$$z = \begin{bmatrix} z_1 \\ z_2 \end{bmatrix}, \quad F_j(z) = \begin{bmatrix} -\frac{1}{n} \sum_i \dot{\ell}(\tilde{r}_i + x_{ij} \tilde{\beta}_j - x_{ij} z_1) x_{ij} + \lambda\alpha z_2 + \lambda(1-\alpha) z_1 \\ z_1 - S(z_1 + z_2) \end{bmatrix}.$$

We solve (3.2) in two corresponding situations as in SNA:

(a) $|\tilde{\beta}_j + \tilde{s}_j| > 1$. For z such that $|z_1 + z_2| > 1$ we have

$$H_j(z) = \begin{bmatrix} \frac{1}{n} \sum_i \ddot{\ell}(\tilde{r}_i + x_{ij}\tilde{\beta}_j - x_{ij}z_1)x_{ij}^2 + \lambda(1-\alpha) & \lambda\alpha \\ 0 & -1 \end{bmatrix} \in \nabla_N F_j(z).$$

The update is

$$\begin{aligned} s_j &\leftarrow \text{sign}(\tilde{\beta}_j + \tilde{s}_j), \\ \beta_j &\leftarrow \tilde{\beta}_j + \frac{\frac{1}{n} \sum_i \dot{\ell}(\tilde{r}_i)x_{ij} - \lambda\alpha s_j - \lambda(1-\alpha)\tilde{\beta}_j}{\frac{1}{n} \sum_i \ddot{\ell}(\tilde{r}_i)x_{ij}^2 + \lambda(1-\alpha)}. \end{aligned}$$

(b) $|\tilde{\beta}_j + \tilde{s}_j| \leq 1$. For z such that $|z_1 + z_2| \leq 1$ we have

$$H_j(z) = \begin{bmatrix} \frac{1}{n} \sum_i \ddot{\ell}(\tilde{r}_i + x_{ij}\tilde{\beta}_j - x_{ij}z_1)x_{ij}^2 + \lambda(1-\alpha) & \lambda\alpha, \\ 1 & 0 \end{bmatrix} \in \nabla_N F_j(z).$$

The update is

$$\begin{aligned} s_j &\leftarrow \frac{\frac{1}{n} \sum_i \dot{\ell}(\tilde{r}_i)x_{ij} + \tilde{\beta}_j \cdot \frac{1}{n} \sum_i \ddot{\ell}(\tilde{r}_i)x_{ij}^2}{\lambda\alpha}, \\ \beta_j &\leftarrow 0. \end{aligned}$$

As described above, our proposed algorithm differs from the previous coordinate descent algorithms (Friedman et al., 2007; Friedman et al., 2010; Simon et al., 2011; Breheny and Huang, 2011) in three important aspects:

- it works for loss functions only first-order differentiable like Huber loss in an elastic-net penalized optimization model;
- the subgradients s_j 's are treated as independent variables which are related to β_j 's through an equation based on the notion of proximity operator;
- each pair of (β_j, s_j) is updated simultaneously with different formulas for two situations $|\tilde{\beta}_j + \tilde{s}_j| > 1$ and $|\tilde{\beta}_j + \tilde{s}_j| \leq 1$. This is quite different from the standard coordinate descent algorithm which only updates the coordinates of the parameter.

3.2 Convergence

SNCD is a special type of coordinate descent algorithm, hence the convergence of the latter as a general framework is of critical importance. The convergence of coordinate descent is proved in a seminal paper by Tseng (2001). Based on the paper, it suffices to show that the optimization problem is of the form

$$\min f(z_1, \dots, z_m) = f_0(z_1, \dots, z_m) + \sum_{j=1}^m f_j(z_j),$$

where f_0, f_1, \dots, f_m are convex, f_0 is first-order differentiable and the level set $\{z : f(z) \leq f(z^0)\}$ is bounded for an initial point z^0 . A key fact to notice about this formulation is that the potentially nondifferentiable part $\sum_j f_j(z_j)$ is separable. Our general model (3.1) apparently satisfies these conditions.

In the updating scheme for each coordinate, SNA is applied to solve the subproblem in each iteration, which requires nonsingularity of the Newton derivative and the uniform boundedness of its inverse. When updating β_0 , these requirements are met if $|\sum_i \ddot{\ell}(y_i - \beta_0 - x_i^\top \beta)|$ is bounded away from 0. When updating β_j , it can be shown via some algebra that a sufficient condition is $0 < \alpha < 1$ and $\ddot{\ell}$ is bounded.

To ensure SNA is convergent for the subproblem in each iteration, we still need to guarantee sufficient closeness between the local starting and optimal points in each iteration. Denote the objective function value at the initial point for (3.1) by f^0 . Since f values decrease along SNCD iterations and the level set $\{(\beta_0, \beta) : f(\beta_0, \beta) \leq f^0\}$ is bounded, the closeness requirement is satisfied if the diameter of the set is sufficiently small.

The above discussions are summarized in the following result.

Theorem 3.1. *For general model (3.1), let $\lambda > 0$, $\alpha \in (0, 1)$ and f value at the initial point be f^0 . Suppose every point (β_0, β) in the level set $\mathcal{L} = \{(\beta_0, \beta) : f(\beta_0, \beta) \leq f^0\}$ satisfies $\sum_i \ddot{\ell}(y_i - \beta_0 - x_i^\top \beta) \geq \delta > 0$ for some δ and $\max_i \ddot{\ell}(y_i - \beta_0 - x_i^\top \beta) \leq M$ for some M . Then SNCD iterations converge to a global minimizer provided that the diameter of \mathcal{L} is sufficiently small.*

3.3 Pathwise Optimization

To successfully apply the algorithm, there is still an important practical issue: a good initial point is required for the algorithm to converge, which is usually unavailable in practice. For low-dimensional problems we can use line search to ensure global convergence with an arbitrary initial point, but since line search methods involve considerable amounts of function and gradient evaluations, they are not well-suited for high-dimensional cases.

Pathwise optimization will serve the role of globalizing the algorithm. With a decreasing sequence of λ values, this strategy sequentially solves the optimization problem at each λ value using the optimizer at the previous one as the initial point. For convex optimization problems, the solution paths are continuous. So when λ, λ' are sufficiently close, $(\hat{\beta}_0(\lambda), \hat{\beta}(\lambda))$ and $(\hat{\beta}_0(\lambda'), \hat{\beta}(\lambda'))$ are close too. In this way, each optimization along the path is warm-started with a good initial point and hence convergence is achieved. In addition, the solution path generated with this strategy is essential in parameter tuning.

Our public R package `hqreg` implements pathwise optimization for SNCD. As a comparison, pathwise optimization for SNA was implemented in another package `huberreg`.

In our implementation, the λ sequence is internally generated to maximize the benefit of warm-start. In particular, λ_0 is chosen as the smallest λ value such that $\hat{\beta}(\lambda) = 0$ for $\lambda \geq \lambda_0$. Having chosen λ_0 , we generate an exponentially decreasing sequence of λ 's and solve the problem at every λ . Table 1 compares timing performance of the two algorithms on a simple example, and SNCD is about 8 times as fast as SNA in this case. Only Huber loss is considered here, for which the algorithmic details are introduced next.

Algorithm	Time
SNA	4.91
SNCD	0.64

Table 1: Total time(in seconds) on Example 1 for 100 λ values, averaged over 3 runs, using $\gamma = 0.2, \alpha = 0.9$.

Example 1. We generate Gaussian data consisting of 500 observations and 2000 predictors, where each pair of predictors has the same population correlation $\rho = 0.2$, and the outcome y_i 's are generated by $y_i = 10 + x_i^\top \beta + \varepsilon_i$, where ε_i 's are iid sampled from Student's t distribution with $df = 5$. We randomly set 50 coefficients to be nonzero and select their values uniformly from $\{\pm 1, \dots, \pm 10\}$.

3.4 SNCD for Penalized Huber Loss Regression

Let $\ell(t) = h_\gamma(t)$. With $\dot{\ell}$ and $\ddot{\ell}$ replaced by \dot{h}_γ and ψ_γ respectively, the SNCD iterations are as follows

i. For the intercept β_0 :

$$\beta_0 \leftarrow \tilde{\beta}_0 + \frac{\sum_i \dot{h}_\gamma(\tilde{r}_i)}{\sum_i \psi_\gamma(\tilde{r}_i)}. \quad (3.3)$$

ii. For each $\beta_j, 1 \leq j \leq p$:

(a) If $|\tilde{\beta}_j + \tilde{s}_j| > 1$, then

$$\begin{aligned} s_j &\leftarrow \text{sign}(\tilde{\beta}_j + \tilde{s}_j), \\ \beta_j &\leftarrow \tilde{\beta}_j + \frac{\frac{1}{n} \sum_i \dot{h}_\gamma(\tilde{r}_i) x_{ij} - \lambda \alpha s_j - \lambda(1 - \alpha) \tilde{\beta}_j}{\frac{1}{n} \sum_i \psi_\gamma(\tilde{r}_i) x_{ij}^2 + \lambda(1 - \alpha)}. \end{aligned} \quad (3.4)$$

(b) If $|\tilde{\beta}_j + \tilde{s}_j| \leq 1$, then

$$\begin{aligned} s_j &\leftarrow \frac{\frac{1}{n} \sum_i \dot{h}_\gamma(\tilde{r}_i) x_{ij} + \tilde{\beta}_j \cdot \frac{1}{n} \sum_i \psi_\gamma(\tilde{r}_i) x_{ij}^2}{\lambda \alpha}, \\ \beta_j &\leftarrow 0. \end{aligned} \quad (3.5)$$

Recalling that $\psi_\gamma(t) = I(|t| \leq \gamma)/\gamma$, we obtain the following result from Theorem 3.1.

Corollary 3.2. *For elastic-net penalized Huber loss regression model, let $\lambda > 0$, $\alpha \in (0, 1)$ and f value at the initial point be f^0 . If for every point (β_0, β) in the level set $\mathcal{L} = \{(\beta_0, \beta) : f(\beta_0, \beta) \leq f^0\}$ there is an $i \in \{1, \dots, n\}$ that satisfies $|y_i - \beta_0 - x_i^\top \beta| \leq \gamma$. Then SNCD iterations converge to a global minimizer provided that the diameter of \mathcal{L} is sufficiently small.*

3.5 SNCD for Penalized Quantile Regression

We cannot apply SNCD directly since ρ_τ is not first-order differentiable. But note

$$\rho_\tau(t) = (1 - \tau)t_- + \tau t_+ = \frac{1}{2} \{ |t| + (2\tau - 1)t \}.$$

Since $h_\gamma(t) \rightarrow |t|$ as $\gamma \rightarrow 0^+$, $\rho_\tau(t) \approx \frac{1}{2} \{ h_\gamma(t) + (2\tau - 1)t \}$ for small γ and the solutions to penalized quantile regression can be approximated by

$$\min_{\beta_0, \beta} f_{RA}(\beta_0, \beta) = \frac{1}{2n} \sum \{ h_\gamma(y_i - \beta_0 - x_i^\top \beta) + (2\tau - 1)(y_i - \beta_0 - x_i^\top \beta) \} + \lambda P_\alpha(\beta), \quad (3.6)$$

which is much more tractable. And as shown later in section 5, the solutions of the above problem converge to a minimizer of the penalized quantile regression as $\gamma \rightarrow 0^+$.

SNCD can be applied to $f_{RA}(\beta_0, \beta)$ with very similar formulas as the ones for Huber loss. At each iteration, denote the current estimates by $(\tilde{\beta}_0, \tilde{\beta})$, then the SNCD updates are

(i) For the intercept β_0 :

$$\beta_0 \leftarrow \tilde{\beta}_0 + \frac{\sum_i \{ \dot{h}_\gamma(\tilde{r}_i) + 2\tau - 1 \}}{\sum_i \psi_\gamma(\tilde{r}_i)}.$$

(ii) For each $\beta_j, j > 0$:

(a) If $|\tilde{\beta}_j + \tilde{s}_j| > 1$, then

$$\begin{aligned} s_j &\leftarrow \text{sign}(\tilde{\beta}_j + \tilde{s}_j), \\ \beta_j &\leftarrow \tilde{\beta}_j + \frac{\frac{1}{2n} \sum_i \{ \dot{h}_\gamma(\tilde{r}_i) + 2\tau - 1 \} x_{ij} - \lambda \alpha s_j - \lambda(1 - \alpha) \tilde{\beta}_j}{\frac{1}{2n} \sum_i \psi_\gamma(\tilde{r}_i) x_{ij}^2 + \lambda(1 - \alpha)}. \end{aligned}$$

(b) If $|\tilde{\beta}_j + \tilde{s}_j| \leq 1$, then

$$\begin{aligned} s_j &\leftarrow \frac{\frac{1}{2n} \sum_i \{ \dot{h}_\gamma(\tilde{r}_i) + 2\tau - 1 \} x_{ij} + \tilde{\beta}_j \cdot \frac{1}{2n} \sum_i \psi_\gamma(\tilde{r}_i) x_{ij}^2}{\lambda \alpha}, \\ \beta_j &\leftarrow 0. \end{aligned}$$

Similar to Corollary 3.2, we have the following result.

Corollary 3.3. *For model (3.6), let $\lambda > 0$, $\alpha \in (0, 1)$ and f value at the initial point be f^0 . If for every point (β_0, β) in the level set $\mathcal{L} = \{(\beta_0, \beta) : f(\beta_0, \beta) \leq f^0\}$ there is an $i \in \{1, \dots, n\}$ that satisfies $|y_i - \beta_0 - x_i^\top \beta| \leq \gamma$. Then SNCD iterations converge to a global minimizer provided that the diameter of \mathcal{L} is sufficiently small.*

For this approximation model to work well, we need to use a sufficiently small γ ; but it cannot be too small, since otherwise we risk having zero as denominators in the updates which leads to divergence. For numerical stability, the scale of γ should be data-dependent too. Therefore, in our implementation of pathwise optimization, we determinate γ depending on the current values of residuals \tilde{r}_i 's and regularization parameter λ_k as follows:

For λ_0 , let $\tilde{r}_i \leftarrow y_i$;

For λ_k ,

- (a) $\gamma_k \leftarrow$ 10-th percentile of $\{|\tilde{r}_i|\}$;
- (b) $\gamma_k \leftarrow \min\{\gamma_k, \gamma_{k-1}\}$;
- (c) $\gamma_k \leftarrow \max\{\gamma_k, 0.0001\}$;
- (d) solve the problem with γ_k, λ_k and keep \tilde{r}_i 's up-to-date.

In (a), the basic idea is to pick a value smaller than the magnitudes of most residuals so that the approximation works well, but it is not too small so that a certain portion of residuals remain below this γ value, which ensures that the denominators in the updates are nonzero. Besides, bracketing in (b) and (c) maintains a trade-off between stability and approximation accuracy. Since our implementation uses a lower bound 0.0001 for γ , for extreme cases we suggest normalizing the responses before fitting the model.

4 The Adaptive Strong Rule for Screening Predictors

Tibshirani et al. (2012) proposed the (sequential) strong rule for screening predictors in pathwise optimization of penalized regression models for computational efficiency. However, when applied to penalized Huber loss regression, we have found that it suffers from the issue of “many violations”, due to the fact that the KKT conditions are more complex. This will be further explained below. To address this issue and enhance algorithmic stability, we propose an adaptive version of the strong rule.

First consider the strong rule for the general elastic-net penalized convex optimization model for regression

$$\min L(\beta_0, \beta) + \lambda \left(\alpha \|\beta\|_1 + (1 - \alpha) \frac{1}{2} \beta^\top \beta \right).$$

Given λ , the optimizer $(\hat{\beta}_0(\lambda), \hat{\beta}(\lambda))$ satisfies the KKT conditions

$$\begin{aligned} \nabla_{\beta_0} L(\hat{\beta}_0, \hat{\beta}) &= 0, \\ \nabla_{\beta_j} L(\hat{\beta}_0, \hat{\beta}) + \lambda \alpha s_j + \lambda(1 - \alpha) \hat{\beta}_j &= 0, \\ \text{where } s_j \in \partial |\hat{\beta}_j|, \quad j &= 1, \dots, p. \end{aligned}$$

The unpenalized intercept β_0 is always in the model, so we use no rule for it. For β_j , let $c_j(\lambda) = \nabla_{\beta_j} L(\hat{\beta}_0(\lambda), \hat{\beta}(\lambda))$. Assume each c_j is α -Lipschitz continuous,

$$|c_j(\lambda) - c_j(\lambda')| \leq \alpha |\lambda - \lambda'|, \quad \text{for every } \lambda, \lambda' > 0. \quad (4.1)$$

Then for pathwise optimization, given $(\hat{\beta}_0(\lambda_{l-1}), \hat{\beta}(\lambda_{l-1}))$ and hence $c_j(\lambda_{l-1})$, the strong rule discards predictor j for λ_l if

$$|c_j(\lambda_{l-1})| < \alpha(2\lambda_l - \lambda_{l-1}). \quad (4.2)$$

This is because, given (4.1) (4.2) and noticing $\lambda_{l-1} > \lambda_l$,

$$\begin{aligned} |c_j(\lambda_l)| &\leq |c_j(\lambda_l) - c_j(\lambda_{l-1})| + |c_j(\lambda_{l-1})| \\ &< \alpha(\lambda_{l-1} - \lambda_l) + \alpha(2\lambda_l - \lambda_{l-1}) \\ &= \alpha\lambda_l. \end{aligned}$$

It follows that $\hat{\beta}_j(\lambda_l) = 0$, as $\hat{\beta}_j(\lambda_l) \neq 0$ if and only if $s_j = \text{sign}(\hat{\beta}_j(\lambda_l))$, which implies that $|c_j(\lambda_l)| = |\lambda_l \alpha \text{sign}(\hat{\beta}_j(\lambda_l)) + \lambda_l(1 - \alpha) \hat{\beta}_j(\lambda_l)| = \lambda_l \alpha + \lambda_l(1 - \alpha) |\hat{\beta}_j(\lambda_l)| \geq \lambda_l \alpha$.

The effectiveness of the strong rule relies on the assumption (4.1). But this assumption can be violated. Thus the application of this rule is accompanied with a check of the KKT conditions. A pathwise optimization algorithm combined with the strong rule proceeds as follows.

For each λ_l , given $c_j(\lambda_{l-1})$'s computed at previous λ_{l-1} ,

- (a) Compute the eligible set $E = \{j : |c_j(\lambda_{l-1})| \geq \alpha(2\lambda_l - \lambda_{l-1})\}$;
- (b) Solve the problem using only predictors in E ;
- (c) Check KKT conditions on the solution: $|c_j(\lambda_l)| \leq \alpha\lambda_l$ for $j \notin E$. We are done if there are no violations; otherwise, add violating indices to E , and repeat steps (b) and (c).

The occurrence of violations appears to be rare for penalized least squares and logistic regressions, but it is a different story for penalized Huber loss regression. In numerical experiments, we often encounter a large number of violations. The reason is that the rule is too restrictive so that at certain λ values many predictors with nonzero coefficients were excluded incorrectly. Since at each λ the algorithm has to be re-run each time violations are found, this substantially increase the computational expenses. Therefore, reducing the number of violations can enhance the algorithmic stability and lead to potential speedup.

A simple approach is to use a multiplier $M > 1$ and relax the assumption (4.1) to $\forall \lambda, \lambda' > 0$,

$$|c_j(\lambda) - c_j(\lambda')| \leq \alpha M |\lambda - \lambda'|.$$

Accordingly, we change the rule (4.2) to

$$|c_j(\lambda_{l-1})| < \alpha (\lambda_l + M(\lambda_l - \lambda_{l-1})).$$

However, this strategy does not work well in practice, since it is difficult to find an M that works for all values of λ in the solution path.

So we allow M to vary with λ and propose an adaptive strong rule. It automatically learns about a localized $M(\lambda)$ that varies and adapts to the trends of the solution paths. The idea is as follows.

Let $M(\lambda_0) = 1$. Then at each λ_l ,

(a) use $M(\lambda_{l-1})$ to construct the eligible set, i.e. let

$$E = \{j : |c_j(\lambda_{l-1})| \geq \alpha (\lambda_l + M(\lambda_{l-1})(\lambda_l - \lambda_{l-1}))\};$$

(b) solve the problem using only the predictors in E , and check KKT conditions as before; update E and repeat step (b) if violations occur;

(c) compute $M(\lambda_l)$ based on the local shape of c_j 's:

$$M(\lambda_l) = \frac{\max_{1 \leq j \leq p} |c_j(\lambda_{l-1}) - c_j(\lambda_l)|}{\alpha(\lambda_{l-1} - \lambda_l)}.$$

We compared how the screening rules perform on the data of example 1. As shown in the following table, both rules help reduce the running time by a large margin. And using adaptive strong rule does help SNCD to get even faster than using the original strong rule by reducing violations.

Algorithm	Time	# violations
SNCD(no screening)	0.64	-
SNCD + Strong Rule	0.18	10
SNCD + Adaptive Strong Rule	0.15	0

Table 2: Total time(in seconds) on example 1 for 100 λ values, averaged over 3 runs, using $\gamma = 0.2, \alpha = 0.9$.

5 Connections between Huber Loss and Quantile, LAD and LS Regression under a Common Penalty

To simplify notation, let $\theta = (\beta_0, \beta)$ and let $P(\cdot)$ be a general penalty function.

5.1 Huber Loss, LAD and LS Regression

We first discuss the connections between P -penalized Huber loss, LAD and LS regression models with the following notations

$$\min_{\theta} f_H(\theta; \lambda, \gamma) = \frac{1}{n} \sum_i h_{\gamma}(y_i - \beta_0 - x_i^{\top} \beta) + \lambda P(\beta),$$

$$\min_{\theta} f_A(\theta; \lambda) = \frac{1}{n} \sum_i |y_i - \beta_0 - x_i^{\top} \beta| + \lambda P(\beta),$$

$$\min_{\theta} f_S(\theta; \lambda) = \frac{1}{2n} \sum_i (y_i - \beta_0 - x_i^{\top} \beta)^2 + \lambda P(\beta).$$

Recall that Huber loss h_{γ} includes the squared and the absolute loss function as the two extremes of $0 < \gamma < \infty$: as $\gamma \rightarrow 0$, $h_{\gamma}(t) \rightarrow |t|$; as $\gamma \rightarrow \infty$, $\gamma h_{\gamma}(t) \rightarrow t^2/2$. It follows that $f_H(\theta; \lambda, \gamma) \rightarrow f_A(\theta; \lambda)$ as $\gamma \rightarrow 0$; $\gamma f_H(\theta; \lambda/\gamma, \gamma) \rightarrow f_S(\theta; \lambda)$ as $\gamma \rightarrow \infty$. Thus it is natural to think there exist inherent connections between their minimizers, which is indeed true as stated in the following theorems.

Theorem 5.1. *Given λ , for any $\{\gamma_k\}$ that tends to 0, let θ_k be a minimizer of $f_H(\theta; \lambda, \gamma_k)$. Then every cluster point of sequence $\{\theta_k\}$ is a minimizer of $f_A(\theta; \lambda)$.*

Theorem 5.2. *Given λ , for any $\{\gamma_k\}$ that tends to ∞ , let θ_k be a minimizer of $f_H(\theta; \lambda/\gamma_k, \gamma_k)$. Then every cluster point of sequence $\{\theta_k\}$ is a minimizer of $f_S(\theta; \lambda)$.*

Thus the penalized Huber loss regression bridges the gap between LAD and LS regression as γ varies from 0 to ∞ . The solutions of penalized Huber loss regression constitute a rich spectrum from the solution of LAD to that of LS. This gives us more flexibility in fitting high-dimensional linear models.

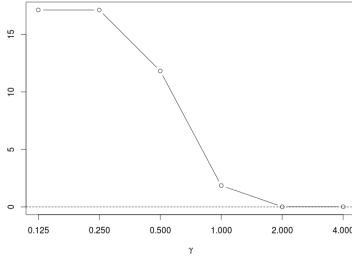


Figure 1: Plot of difference between solutions of penalized Huber loss and LS regressions. The y-axis measures $\|\hat{\theta}_H(0.1/\gamma, \gamma) - \hat{\theta}_S(0.1)\|_2$.

Again, we use data of Example 1 to demonstrate the convergence empirically. We used our R package `hqreg` to compute $\hat{\theta}_H$'s and another package `glmnet` for $\hat{\theta}_S$, where $\hat{\theta}_H$ and $\hat{\theta}_S$ denote minimizers of f_H and f_S respectively. Since `glmnet` internally scales the response by its standard deviation to fit the model, to compare the results we first scaled Y and ran the programs, and then unscaled the resulting coefficients. Using $\lambda = 0.1, \alpha = 0.9$, we computed the solution to penalized LS regression $\hat{\theta}_S(0.1)$ and solutions for penalized Huber loss regression $\hat{\theta}_H(0.1/\gamma, \gamma)$ along an increasing sequence of γ . The plot of $\|\hat{\theta}_H(0.1/\gamma, \gamma) - \hat{\theta}_S(0.1)\|_2$ against γ values is shown in Figure 1, revealing that the difference shrinks to zero as γ increases.

5.2 Huber Loss and Quantile Regression

Now consider the P -penalized quantile regression

$$\min_{\theta} f_Q(\theta; \lambda, \tau) = \frac{1}{n} \sum_i \rho_{\tau}(y_i - \beta_0 - x_i^{\top} \beta) + \lambda P(\beta). \quad (5.1)$$

As before, rewrite the quantile loss function

$$\rho_{\tau}(t) = \frac{1}{2} \{ |t| + (2\tau - 1)t \}.$$

Thus the above problem can be approximated by

$$\min_{\theta} f_{RA}(\theta; \lambda, \tau, \gamma) = \frac{1}{2n} \sum_i \{ h_{\gamma}(y_i - \beta_0 - x_i^{\top} \beta) + (2\tau - 1)(y_i - \beta_0 - x_i^{\top} \beta) \} + \lambda P(\beta), \quad (5.2)$$

where ‘‘RA’’ stands for robust approximation because here we use Huber loss to approximate the absolute loss. The following result provides theoretical support for such an approximation.

Theorem 5.3. Given λ and τ , for any $\{\gamma_k\}$ that tends to 0, let θ_k be a minimizer of $f_{RA}(\theta; \lambda, \tau, \gamma_k)$. Then every cluster point of sequence $\{\theta_k\}$ is a minimizer of $f_Q(\theta; \lambda, \tau)$.

6 Optimization Performance for Penalized Quantile Regression

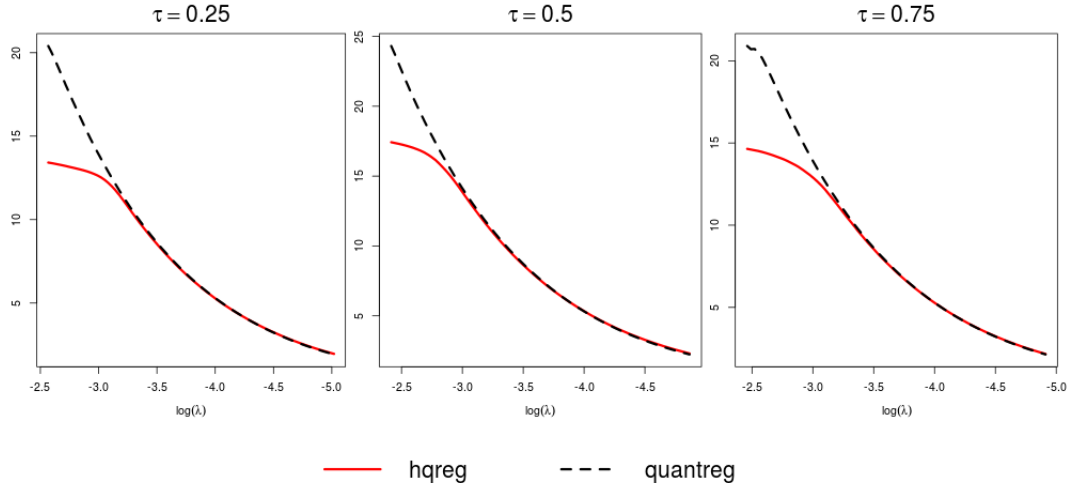


Figure 2: Values of objective functions for penalized quantile regression on Example 1, evaluated for an entire solution path.

Aside from our package `hqreg`, to the best of our knowledge, `quantreg` is the only other R package that supports ℓ_1 penalized quantile regression that is publicly available and well documented. Since our implementation uses an approximation model at every λ , we benchmark our solutions against the ones computed with `quantreg` in terms of optimality, which is done by comparing the objective function values (f_Q) at each λ .

However, unlike `hqreg`, `quantreg` does not compute an entire solution path but only a single solution for a given λ value. Also it does not support the general elastic-net penalty with $\alpha < 1$. In order to compare performances of the two packages, we set $\alpha = 1$ and choose $\tau = 0.25, 0.50, 0.75$. For each τ , we first compute an entire solution path for 100 λ values using `hqreg`, then run `quantreg` at each λ .

For Example 1, the comparisons for all 3 cases are shown in Figure 2. It appears that the optimization performance of `hqreg` is at least as good as that of `quantreg` and surprisingly outperforms the latter for larger λ values.

We also compare their computing time in Table 3. The time for `quantreg` is the sum of time used on each λ . In this case, the advantage of `hqreg` is very significant. It is over 100 times faster than `quantreg`.

τ	<code>hqreg</code>	<code>quantreg</code>
0.25	27.88	6698.89
0.50	16.20	6821.14
0.75	36.35	6447.08

Table 3: Timings (in seconds) for computing regularization paths for quantile regression with elastic-net penalty on Example 1. Total time for 100 λ values.

Example 2. Generate 10000 simulated datasets using the settings of Example 1, except that the number of observations n and the number of predictors p are randomly chosen from the set $\{20, 100, 200, 500, 1000, 2000, 5000\}$, and the percentage of nonzero coefficients is randomly chosen from the set $\{2.5\%, 5\%, 10\%, 20\%\}$.

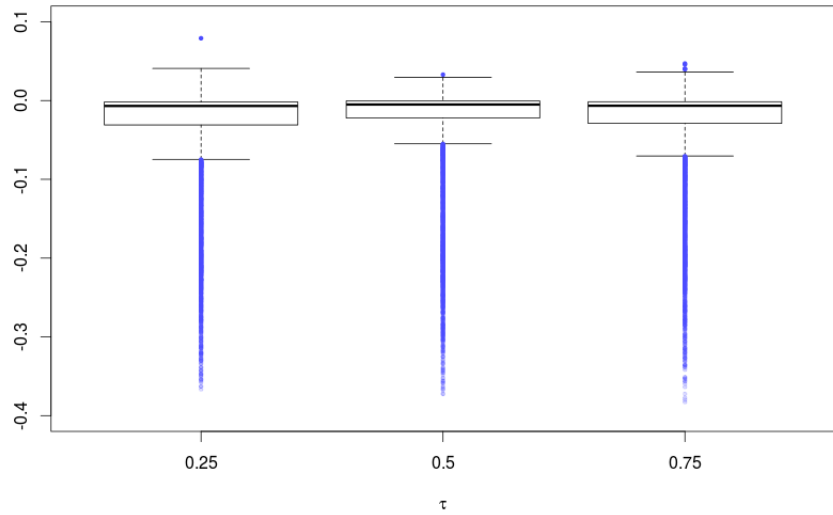


Figure 3: Boxplot of relative differences of objective function values with different τ 's on 10000 simulated datasets of Example 2.

To investigate performances of `hqreg` in different situations, we ran a large-scale experiment as described in Example 2. For each dataset and each τ , we used `hqreg` to compute an entire solution path and chose an index k out of $\{10, 20, \dots, 100\}$, then ran `quantreg`

to compute the solution at λ_k , the k -th element of the sequence of λ 's. At the end, we computed the relative difference of objective function values evaluated at the two solutions, i.e.

$$\frac{f_Q(\hat{\beta}_{hqreg}) - f_Q(\hat{\beta}_{quantreg})}{f_Q(\hat{\beta}_{quantreg})}$$

where f_Q represents the objective function of penalized quantile regression, $\hat{\beta}_{hqreg}$ and $\hat{\beta}_{quantreg}$ represent the solutions computed by `hqreg`, `quantreg` respectively. The results are summarized via three boxplots (Figure 3). We can see that

- most values are between 0.1 and -0.1, showing that the performances of the two packages are generally close;
- there is no value exceeding 0.1, while there is a considerable amount below -0.1, which means `hqreg` performs better than `quantreg` in some cases.

These results provide strong evidence that `hqreg` is at least as good as `quantreg` in optimization performance, and can perform much better in some cases.

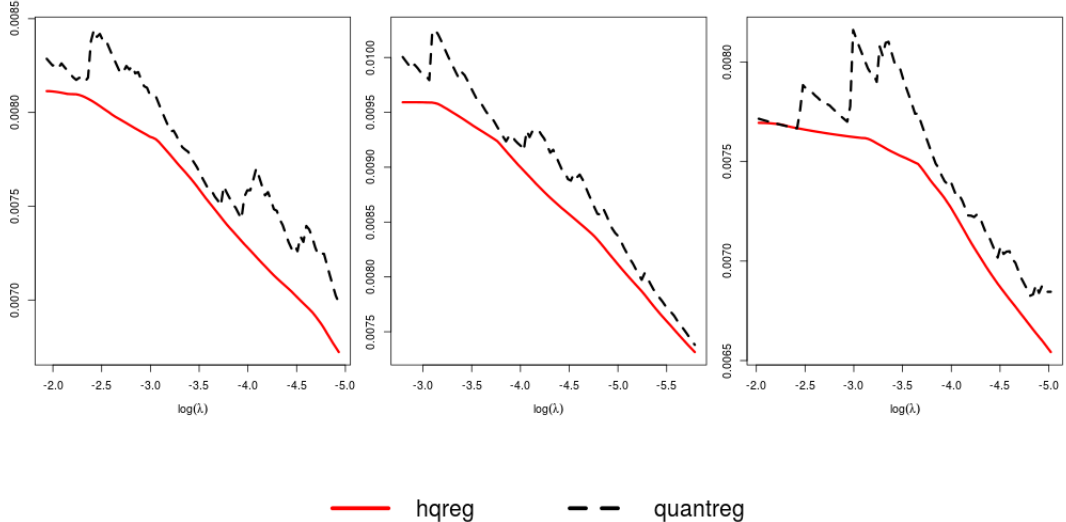


Figure 4: Values of objective functions evaluated at each λ along the solution path for `barro` dataset. From left to right: $\tau = 0.25, 0.50, 0.75$.

We also compared the two packages on a real dataset `barro` from package `quantreg`. The dataset was originally taken from Barro and Lee (1994) and used in Koenker and Machado (1999) to illustrate methods for inference on quantile regression. The data consists

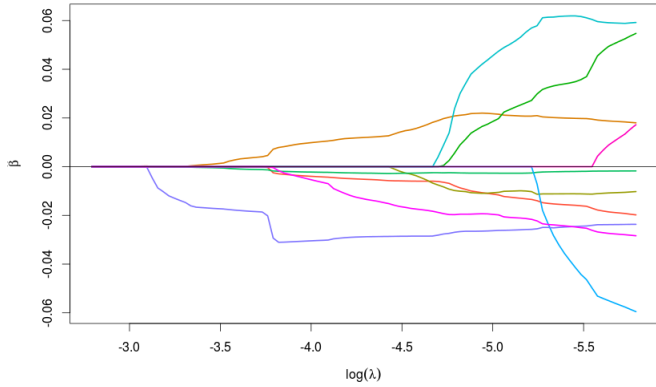


Figure 5: Regularization path for quantile regression with $\tau = 0.5$ on `barro` dataset, computed by `hqreg`.

of 161 observations on national GDP growth rates, recorded as “Annual Change Per Capita GDP”, and contains 13 other covariates as predictors. The first 71 observations are on the period 1965-1975, and the rest are on the period 1975-1985. Figure 4 shows that `hqreg` outperforms `quantreg` for all three τ values.

Take a further look at the solutions themselves, we found that there is yet another important distinction between the solutions computed by the two packages. While `hqreg` automatically yields sparse solutions, `quantreg` does not. All the coefficients computed by `quantreg` are nonzero, no matter what λ value is used. For `hqreg`, however, while there are 10 nonzero coefficients at λ_{100} , there is none except the unpenalized intercept at λ_1 . The sparse solutions given by `hqreg` is naturally more interpretable. Also, with the solution paths plotted by `hqreg` as shown in Figure 5, we can see more clearly λ ’s impact on sparsity of the solutions. One may argue that thresholding can be used to screen out coefficients close to zero for the solutions given by `quantreg`. But taking this dataset for example, from Figure 5 we can see that the solutions have very small values, which makes thresholding difficult. In high-dimensional settings, this difference can be crucial.

7 Timing Performance

7.1 Elastic-Net Penalized Huber Loss Regression and LS Regression

In this part, we compare the running times of competing methods for elastic-net penalized Huber loss and LS regression. As far as we know, SNA and SNCD proposed in this paper are the only ones available that compute solution paths for penalized Huber loss regression. Hence, the candidates for Huber loss are SNA, SNCD with no screening(SNCD), SNCD with strong rule(SNCD+SR), and SNCD with adaptive strong rule(SNCD+ASR). Since our SNCD implementation in `hqreg` supports the squared loss, it would be also interesting to see how it compares with state-of-the-art R package `glmnet`, which computes solution paths for elastic-net penalized GLMs. `hqreg` supports the 3 different screening strategies via one argument(`screen` = “none”, “SR”, “ASR”). For `glmnet`, the latest version `glmnet_2.0-2` was used, which also employs the strong rule. As mentioned before, `glmnet` scales the responses automatically to have unit variance. To compare timing performances fairly, we used scaled responses for each dataset.

We generated Gaussian data with N observations and P predictors, where each pair of predictors have an identical correlation ρ . To simplify settings and highlight the timing comparison based on the key parameter γ , we set $\rho = 0.2$ for all data. The responses were generated by

$$Y = \sum_j X_j \beta_j + k \cdot E$$

where $\beta_j = (-1)^j \exp(-(j-1)/10)$, $E \sim T(df = 4)$ and k is determined so that the signal-to-noise ratio is 3. The coefficients were constructed to have alternating signs with magnitude exponentially decreasing to 0. And the error terms E were designed to have moderate tail behavior that characterize most real world data. After generation, the responses are scaled by standard deviation to fit the models. After examining descriptive statistics of the scaled responses, we decided to use $\gamma = 0.01, 0.1, 1, 10, 100$ for Huber loss. We set $\alpha = 0.9$ in all cases.

In practice, we have found that convergence of SNA has much higher dependence on the closeness of initial points to the optimizers than SNCD. Therefore, we divided the experiments into two parts. In the first part, we compared SNCD, SNCD+SR, SNCD+ASR, leaving out SNA, for Huber loss on a sequence of 100 lambda values, and then also compared these algorithms with `glmnet` for the least squares. In the second part, we compared only SNA and SNCD for Huber loss on a dense lambda sequence consisting of 10000 values.

Table 4 shows average CPU timings for the first part. First compare the timings for

	Huber					Squared
	0.01	0.1	1	γ	100	
$N = 1000, P = 100$						
SNCD	0.15	0.06	0.05	0.04	0.04	0.03
SNCD+SR	0.09(10)	0.04(2)	0.03(0)	0.03(0)	0.03(0)	0.02(0)
SNCD+ASR	0.09(2)	0.04(1)	0.03(0)	0.03(0)	0.02(0)	0.02(0)
glmnet	—	—	—	—	—	0.01
$N = 5000, P = 100$						
SNCD	0.47	0.29	0.23	0.21	0.21	0.15
SNCD+SR	0.31(4)	0.18(0)	0.13(0)	0.15(0)	0.12(0)	0.08(0)
SNCD+ASR	0.31(3)	0.18(0)	0.12(0)	0.12(0)	0.12(0)	0.08(0)
glmnet	—	—	—	—	—	0.02
$N = 100, P = 1000$						
SNCD	2.00	0.47	0.11	0.10	0.10	0.05
SNCD+SR	0.52(35)	0.12(17)	0.03(0)	0.03(0)	0.03(0)	0.02(0)
SNCD+ASR	0.64(1)	0.14(1)	0.03(0)	0.03(0)	0.03(0)	0.02(0)
glmnet	—	—	—	—	—	0.02
$N = 100, P = 5000$						
SNCD	9.74	2.38	0.56	0.45	0.46	0.28
SNCD+SR	0.77(22)	0.24(4)	0.11(0)	0.11(0)	0.11(0)	0.10(0)
SNCD+ASR	1.12(0)	0.29(0)	0.12(0)	0.11(0)	0.11(0)	0.08(0)
glmnet	—	—	—	—	—	0.11
$N = 100, P = 20000$						
SNCD	37.25	9.47	2.36	2.29	2.30	1.23
SNCD+SR	1.28(8)	0.60(4)	0.42(1)	0.42(0)	0.41(0)	0.31(0)
SNCD+ASR	1.86(1)	0.71(1)	0.44(1)	0.43(0)	0.43(0)	0.32(0)
glmnet	—	—	—	—	—	0.33
$N = 100, P = 50000$						
SNCD	97.35	22.56	5.10	5.06	5.10	3.66
SNCD+SR	2.58(9)	1.23(1)	0.96(0)	0.95(1)	0.96(1)	0.98(0)
SNCD+ASR	3.61(1)	1.39(0)	1.00(0)	1.00(1)	1.00(1)	1.02(0)
glmnet	—	—	—	—	—	0.76

Table 4: Timings (in seconds) for computing regularization paths for Huber loss and least squares regression with elastic-net penalty. Total time for 100 λ values, averaged over 3 runs. Numbers in the parentheses are total times of violations, only applicable to SNCD with strong rule or adaptive strong rule.

Huber loss. Across different values of γ , we see that the timings for the three versions of SNCD all increase when γ is nearing 0, and are almost the same for $\gamma \geq 1$. Comparing different algorithms for penalized Huber loss regression, we see that employing the strong rule or the adaptive strong rule in SNCD reduces time by a large margin and scales much better with dimensions in comparison to SNCD with no screening; between the two the timings are close, differing mainly in that **SNCD+ASR** encounters much fewer violations.

	γ		
	0.01	1	10
$N = 1000, P = 100$			
SNA	3.98	5.16	5.44
SNCD	3.32	3.53	3.41
$N = 5000, P = 100$			
SNA	17.98	24.42	26.33
SNCD	20.98	17.83	17.11
$N = 100, P = 1000$			
SNA	×	11.70	10.47
SNCD	3.68	3.45	3.43
$N = 100, P = 5000$			
SNA	×	98.66	100.76
SNCD	13.04	12.58	12.51

Table 5: Timings (in seconds) for computing regularization paths for Huber loss. “ \times ” represents early exit due to divergence at some λ value. Total time for 10000 λ values.

For least squares, **SNCD+SR**, **SNCD+ASR** and **glmnet** have similar performances. Although they are slower when N is relatively large, for the other cases their timings are competitive with **glmnet**. This shows that SNCD is fast in general, not only for Huber loss, but also for the squared loss. Besides, we discover that the timings for Huber and squared loss are mostly comparable. Considering that Huber loss is harder to handle than the simple squared loss, the performance of **hqreg** is impressive.

Table 5 shows average CPU timings for the second part. We have found earlier that SNA tends to diverge for high-dimensional data, and once diverging at a λ it continues to fail at following ones. Hence for this part we add a criterion that either algorithm is forced to stop once divergence is detected. In Table 5 we see that while SNCD has converged in every case, SNA has failed where P is large and $\gamma = 0.1$ is used. When P is small,

SNCD does not seem much faster. When P increases, SNCD shows an increasing speedup compared to SNA and becomes considerably faster. These results show that SNCD is much more stable and scalable than SNA.

7.2 ℓ_1 Penalized Quantile Regression

	τ		
	0.25	0.50	0.75
$N = 1000, P = 100$			
hqreg	0.31	0.29	0.26
quantreg	7.90	7.62	7.58
$N = 5000, P = 100$			
hqreg	0.60	0.71	0.50
quantreg	60.43	59.68	62.21
$N = 100, P = 1000$			
hqreg	39.06	36.10	41.60
quantreg	241.77	218.05	199.22
$N = 100, P = 5000$			
hqreg	51.49	52.93	64.23
quantreg	7840.34	7398.69	7402.34

Table 6: Timings (in seconds) for computing regularization paths for penalized quantile regression. Total time for 100 λ values.

In section 6, we have shown that `hqreg` outperforms `quantreg` in terms of optimality. Also `hqreg` appears to be much faster for Example 1. Here we show more timing comparison on the same simulated datasets used in the first part. As mentioned previously, `quantreg` supports lasso (ℓ_1) but not general elastic-net, so we set $\alpha = 1$.

As shown in Table 6, `hqreg` is considerably faster than `quantreg` in all cases. `hqreg` also shows much better scalability with both N and P . It can be more than 100 times faster in higher dimensional cases, just like Example 1. Finally, it is a little surprising that both packages perform significantly better for cases with small P and large N . Further investigation is necessary to explain the phenomenon.

8 Breast Cancer Gene Expression Data Example

We use the breast cancer data from The Cancer Genome Atlas (2012) project (<http://cancergenome.nih.gov/>) to illustrate the performance of penalized Huber loss regression. We also compare the results with those from the penalized least squares regression. We focus on the gene expression dataset obtained using Agilent mRNA expression microarrays. It contains expression measurements of 17814 genes from 519 patients, including BRCA1, the first gene identified that increases the risk of early onset breast cancer. Hence we regress the key gene BRCA1 on the other genes using the two methods and compare their prediction performance.

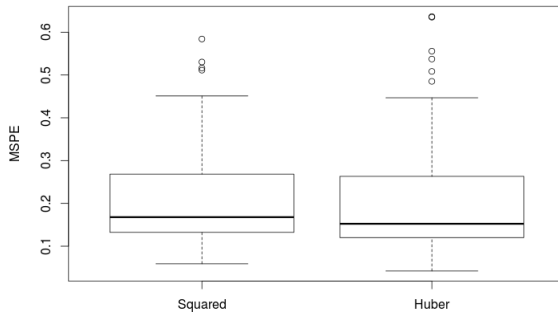


Figure 6: Boxplot of MSPE for the original data.

On each run, we randomly chose 20 patients as the test set, trained models on the rest to obtain coefficient estimates, which in return were used to make prediction on the 20 patients. As before, we used the elastic-net penalty with $\alpha = 0.9$, and after conducting a pilot study we decided to use $\gamma = 1$ for Huber loss. Then the regularization parameter λ 's were chosen via 5-fold cross validation for both methods. We repeated the random splitting 100 times. The boxplots of MSPE in Figure 6 show that Huber loss gives us better predictions than the squared loss under the same elastic-net penalty.

To further study the robustness of Huber loss, we changed the settings by adding mild perturbation to the data and repeated the experiments. We first computed $se(y)$, the standard errors of all the responses. Then for each splitting we randomly chose 10% of the training set and added $5 \cdot se(y)$ to their responses so that they would be outliers. The boxplot of MSPE for this scenario is shown in Figure 7. With this slight perturbation, the advantage of using Huber loss becomes more obvious.

To sum up, these experiments provide evidence that Huber loss regression is very competitive with LS under the same regularization for fitting high-dimensional linear models, because it tends to achieve better modelling performance while maintaining the training

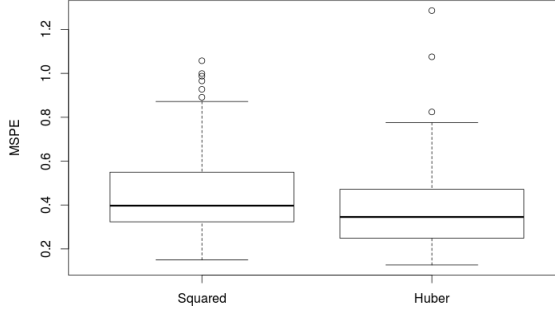


Figure 7: Boxplot of MSPE for the perturbed data.

efficiency of the penalized LS. In section 7, the timing results for multiple scenarios provide more convincing support for the computational efficiency of Huber loss regression.

9 Conclusion

Robust and quantile regression models have important applications in many fields. However, there is a lack of publicly available and well documented software that can fit these models in high-dimensional settings. In this paper, we develop an efficient and scalable algorithm for computing the solution paths for these models with the elastic-net penalty. We also provide an implementation via the R package `hqreg` publicly available on CRAN (<http://cran.r-project.org/web/packages/hqreg/index.html>).

A Appendix

In this appendix, we give detailed proofs of Lemmas 2.4, 2.5 and Theorems 2.6, 5.1, 5.2. The proof of Theorem 5.3 is similar to that of Theorem 5.1 and hence omitted.

Proof of Lemma 2.4.

(i) By assumption, the Jacobian J_F is continuous at z . Since

$$\begin{aligned}
 & \frac{\|F(z+h) - F(z) - J_F(z+h)h\|_2}{\|h\|_2} \\
 & \leq \frac{\|F(z+h) - F(z) - J_F(z)h\|_2 + \|(J_F(z) - J_F(z+h))h\|_2}{\|h\|_2} \\
 & \leq \frac{\|F(z+h) - F(z) - J_F(z)h\|_2}{\|h\|_2} + \|J_F(z) - J_F(z+h)\| \\
 & \rightarrow 0
 \end{aligned}$$

as $h \rightarrow \mathbf{0}$, by definition $J_F \in \nabla_N F(z)$.

(ii)

$$\|AF(z+h) - AF(z) - AH(z+h)h\|_2 \leq \|A\| \|F(z+h) - F(z) - H(z+h)h\|_2 = o(\|h\|_2),$$

hence $AH \in \nabla_N AF(z)$.

(iii)

$$\begin{aligned} & \| (F(z+h) + G(z+h)) - (F(z) + G(z)) - (H_F(z+h) + H_G(z+h))h \|_2 \\ & \leq \|F(z+h) - F(z) - H_F(z+h)h\|_2 + \|G(z+h) - G(z) - H_G(z+h)h\|_2 \\ & = o(\|h\|_2), \end{aligned}$$

hence $H_F + H_G \in \nabla_N (F+G)(z)$.

(iv) It can be seen by observing that

$$\|F(z+h) - F(z) - H(z+h)h\|_2^2 = \sum_{i=1}^l (F_i(z+h) - F_i(z) - H_i(z+h)h)^2.$$

Proof of Lemma 2.5.

If f is differentiable at z with derivative f' defined in its neighborhood, by smoothness assumption and Lemma 2.4(i), $f' \in \nabla_N f(z)$.

If f is not differentiable at z , by assumption there exists $s > 0$ such that f is smooth on both $(z-s, z)$ and $(z, z+s)$ implying that $f'(z-) = \lim_{h \rightarrow 0^-} \frac{f(z+h) - f(z)}{h}$ and $f'(z+) = \lim_{h \rightarrow 0^+} \frac{f(z+h) - f(z)}{h}$ exist and

$$\begin{aligned} f'(z+h) & \rightarrow f'(z-) & \text{as } h \rightarrow 0^-, \\ f'(z+h) & \rightarrow f'(z+) & \text{as } h \rightarrow 0^+. \end{aligned}$$

Hence for any $\varepsilon > 0$, there exists a sufficiently small $\delta > 0$ such that

$$\begin{aligned} \forall x \in (z-\delta, z), \quad & \frac{|f(x) - f(z) - f'(z-)(x-z)|}{|x-z|} < \varepsilon/2, \quad |f'(x) - f'(z-)| < \varepsilon/2; \\ \forall x \in (z, z+\delta), \quad & \frac{|f(x) - f(z) - f'(z+)(x-z)|}{|x-z|} < \varepsilon/2, \quad |f'(x) - f'(z+)| < \varepsilon/2. \end{aligned}$$

Thus for $x \in (z-\delta, z)$,

$$\frac{|f(x) - f(z) - f'(x)(x-z)|}{|x-z|} \leq \frac{|f(x) - f(z) - f'(z-)(x-z)|}{|x-z|} + |f'(z-) - f'(x)| < \varepsilon,$$

and similarly for $x \in (z, z+\delta)$. Define $H(z)$ as in the lemma, then the above implies

$$\forall \varepsilon > 0, \exists \delta > 0 \text{ s.t. } \forall |x-\delta| < z, \quad \frac{|f(x) - f(z) - H(x)(x-z)|}{|x-z|} < \varepsilon.$$

In other word, f is Newton differentiable at z with $H \in \nabla_N f(z)$.

Proof of Theorem 2.6.

Notice \mathcal{S} is piecewise-smooth, then by Lemma 2.3, 2.5 and Lemma 2.4 (iv) $F_1(Z)$ is Newton differentiable, and with (2.8)

$$\begin{bmatrix} -I_{|A|} & \mathbf{0} & 0 & \mathbf{0} & \mathbf{0} \\ \mathbf{0} & I_{|B|} & 0 & \mathbf{0} & \mathbf{0} \end{bmatrix} \in \nabla_N F_1(Z).$$

Similarly, the Huber loss is also piecewise-smooth, and by Lemma 2.3, 2.5 and Lemma 2.4 (ii)-(iv), we have $F_2(Z)$ and $F_3(Z)$ are Newton differentiable and

$$\begin{bmatrix} \mathbf{0} & \mathbf{1}_n^\top \Psi X_B & \mathbf{1}_n^\top \Psi \mathbf{1}_n & \mathbf{1}_n^\top \Psi X_A & \mathbf{0} \end{bmatrix} \in \nabla_N F_2(Z),$$

$$\begin{bmatrix} \mathbf{0} & \mathbf{1}_n^\top \Psi X_B & \mathbf{1}_n^\top \Psi \mathbf{1}_n & \mathbf{1}_n^\top \Psi X_A & \mathbf{0} \\ \lambda \alpha I_{|A|} & X_A^\top \Psi X_B & X_A^\top \Psi \mathbf{1}_n & X_A^\top \Psi X_A + \lambda(1 - \alpha) I_{|A|} & \mathbf{0} \\ \mathbf{0} & X_B^\top \Psi X_B + \lambda(1 - \alpha) I_{|B|} & X_B^\top \Psi \mathbf{1}_n & X_B^\top \Psi X_A & \lambda \alpha I_{|B|} \end{bmatrix} \in \nabla_N F_3(Z).$$

Again, by Lemma 2.4 (iv), $F(Z)$ is Newton differentiable and

$$H = \begin{bmatrix} -I_{|A|} & \mathbf{0} & 0 & \mathbf{0} & \mathbf{0} \\ \mathbf{0} & I_{|B|} & 0 & \mathbf{0} & \mathbf{0} \\ \mathbf{0} & \mathbf{1}_n^\top \Psi X_B & \mathbf{1}_n^\top \Psi \mathbf{1}_n & \mathbf{1}_n^\top \Psi X_A & \mathbf{0} \\ \lambda \alpha I_{|A|} & X_A^\top \Psi X_B & X_A^\top \Psi \mathbf{1}_n & X_A^\top \Psi X_A + \lambda(1 - \alpha) I_{|A|} & \mathbf{0} \\ \mathbf{0} & X_B^\top \Psi X_B + \lambda(1 - \alpha) I_{|B|} & X_B^\top \Psi \mathbf{1}_n & X_B^\top \Psi X_A & \lambda \alpha I_{|B|} \end{bmatrix} \in \nabla_N F(Z).$$

Now let

$$H_1 = \begin{bmatrix} -I_{|A|} & \mathbf{0} \\ \mathbf{0} & I_{|B|} \end{bmatrix}, \quad H_2 = \begin{bmatrix} \mathbf{0} & \mathbf{1}_n^\top \Psi X_B \\ \lambda \alpha I_{|A|} & X_A^\top \Psi X_B \mathbf{0} X_B^\top \Psi X_B + \lambda(1 - \alpha) I_{|B|} \end{bmatrix},$$

$$H_3 = \begin{bmatrix} \mathbf{1}_n^\top \Psi \mathbf{1}_n & \mathbf{1}_n^\top \Psi X_A & \mathbf{0} \\ X_A^\top \Psi \mathbf{1}_n & X_A^\top \Psi X_A + \lambda(1 - \alpha) I_{|A|} & \mathbf{0} \\ X_B^\top \Psi \mathbf{1}_n & X_B^\top \Psi X_A & \lambda \alpha I_{|B|} \end{bmatrix}. \quad (\text{A.1})$$

Then it is clear that H_1 is invertible. Now if H_3 is also invertible, which we show in Lemma A.1 under a mild condition, then via some algebra we have

$$H^{-1} = \begin{bmatrix} H_1^{-1} & \mathbf{0} \\ -H_3^{-1} H_2 H_1^{-1} & H_3^{-1} \end{bmatrix}. \quad (\text{A.2})$$

Let $g = (g_1^\top, g_2^\top)^\top \in \mathbb{R}^p \times \mathbb{R}^{p+1}$, then

$$\begin{aligned}
\|H^{-1}g\|_2^2 &= \|H_1^{-1}g_1\|_2^2 + \| -H_3^{-1}H_2H_1^{-1}g_1 + H_3^{-1}g_2\|_2^2 \\
&\leq \|H_1^{-1}\|^2\|g_1\|_2^2 + (\|H_3^{-1}\|\|H_2\|\|H_1^{-1}\|\|g_1\|_2 + \|H_3^{-1}\|\|g_2\|_2)^2 \\
&\leq (\|H_1^{-1}\|\|g_1\|_2 + \|H_3^{-1}\|\|H_2\|\|H_1^{-1}\|\|g_1\|_2 + \|H_3^{-1}\|\|g_2\|_2)^2 \\
&\leq (\|H_1^{-1}\| + \|H_3^{-1}\| + \|H_3^{-1}\|\|H_2\|\|H_1^{-1}\|)^2\|g\|_2^2
\end{aligned} \tag{A.3}$$

which implies

$$\|H^{-1}\| \leq \|H_1^{-1}\| + \|H_3^{-1}\| + \|H_3^{-1}\|\|H_2\|\|H_1^{-1}\|. \tag{A.4}$$

Notice $\|X_A\| \vee \|X_B\| \leq \|X\|$. Take X_A , without loss of generality shuffle columns of X such that $X = \begin{pmatrix} X_A & X_B \end{pmatrix}$, then for any $g \in \mathbb{R}^{|A|}$ such that $\|g\|_2 = 1$, we have

$$\|X_Ag\|_2 = \|X \begin{pmatrix} g \\ \mathbf{0} \end{pmatrix}\|_2 \leq \sup \{\|Xv\|_2 : \|v\|_2 = 1\} = \|X\|,$$

implying that $\|X_A\| = \sup \{\|X_Ag\|_2 : \|g\|_2 = 1\} \leq \|X\|$. Similarly for X_B .

Then a similar argument as in (A.3) shows that

$$\|H_2\| \leq 1 + \alpha + 2\|X\|^2 \tag{A.5}$$

Combining (A.4), (A.5) with results of Lemma A.1 under its condition, and observing that $\|H_1^{-1}\| = 1$, we obtain the uniform boundedness of H in spectral norm, i.e.,

$$\begin{aligned}
\|H^{-1}\| &\leq 1 + \left[\frac{1}{\lambda\alpha} + \left(\frac{1}{\lambda(1-\alpha)} + \frac{\lambda_{\max}(X^\top X)^2 + n\gamma\lambda(1-\alpha)}{\lambda(1-\alpha)} \left(1 + \frac{\|X\|}{\sqrt{n}\gamma\lambda(1-\alpha)} \right)^2 \right) \right. \\
&\quad \times \left. \left(1 + \frac{2\|X\|}{\sqrt{n}\gamma\lambda\alpha} \right) \right] (2 + \alpha + 2\|X\|^2).
\end{aligned}$$

The following lemma is used in the proof of Theorem 2.6.

Lemma A.1. *Given $\alpha \in (0, 1)$ and β_0, β satisfy $|y_i - \beta_0 - x_i^\top \beta| \leq \gamma$ for some i , then H_3 in (A.1) is invertible with its inverse uniformly bounded in spectral norm, i.e.*

$$\|H_3^{-1}\| \leq \frac{1}{\lambda\alpha} + \left[\frac{1}{\lambda(1-\alpha)} + \frac{\lambda_{\max}(X^\top X)^2 + n\gamma\lambda(1-\alpha)}{\lambda(1-\alpha)} \left(1 + \frac{\|X\|}{\sqrt{n}\gamma\lambda(1-\alpha)} \right)^2 \right] \left(1 + \frac{2\|X\|}{\sqrt{n}\gamma\lambda\alpha} \right).$$

Proof. The key of this proof is that $\Psi = \frac{1}{n\gamma}J$, where J is diagonal and idempotent.

Then we have

$$\mathbf{1}_n^\top \Psi \mathbf{1}_n = \frac{1}{n\gamma} \mathbf{1}_n^\top J \mathbf{1}_n = \frac{1}{n\gamma} (J \mathbf{1}_n)^\top (J \mathbf{1}_n),$$

and

$$\begin{aligned} & \mathbf{1}_n^\top \Psi X_A \left(X_A^\top \Psi X_A + \lambda(1-\alpha)I_{|A|} \right)^{-1} X_A^\top \Psi \mathbf{1}_n \\ &= \frac{1}{n\gamma} (J\mathbf{1}_n)^\top (JX_A) \left((JX_A)^\top (JX_A) + n\gamma\lambda(1-\alpha)I_{|A|} \right)^{-1} (JX_A)^\top (J\mathbf{1}_n) \end{aligned}$$

Denote $a = J\mathbf{1}_n$, $Z = JX_A$, $t = n\gamma\lambda(1-\alpha)$, and $m = |A|$. Then the LHS becomes

$$\frac{1}{n\gamma} \left(a^\top a - a^\top Z (Z^\top Z + tI_m)^{-1} Z^\top a \right).$$

Since $|y_i - \beta_0 - x_i^\top \beta| \leq \gamma$ for some i , we have $\psi_i = \frac{1}{n\gamma} > 0$, implying that $J_{ii} = 1$ and $a^\top a \geq J_{ii}^2 = 1$. Thus we are guaranteed that $a = J\mathbf{1}_n$ is not a zero vector.

Now apply SVD to Z such that $Z = UDV^\top$, where $U_{n \times n}$ and $V_{m \times m}$ are both orthogonal matrices, and $D_{n \times m}$ is a rectangular diagonal matrix with non-negative diagonal elements $d_1, \dots, d_{m \wedge n}$. Hence

$$\begin{aligned} Z(Z^\top Z + tI_m)^{-1} Z^\top &= UDV^\top (VD^\top U^\top UDV^\top + tI_m)^{-1} VD^\top U^\top \\ &= UDV^\top (V(D^\top D + tI_m)V^\top)^{-1} VD^\top U^\top \\ &= UDV^\top V(D^\top D + tI_m)^{-1} V^\top VD^\top U^\top \\ &= UD(D^\top D + tI_m)^{-1} D^\top U^\top \end{aligned}$$

When $n > m$,

$$D(D^\top D + tI_m)^{-1} D^\top = \text{diag}\left(\frac{d_1^2}{d_1^2 + t}, \dots, \frac{d_m^2}{d_m^2 + t}, 0, \dots, 0\right);$$

when $n \leq m$,

$$D(D^\top D + tI_m)^{-1} D^\top = \text{diag}\left(\frac{d_1^2}{d_1^2 + t}, \dots, \frac{d_n^2}{d_n^2 + t}\right).$$

In either case $D(D^\top D + tI_m)^{-1} D^\top$ is p.s.d. with $\lambda_{\max}(D(D^\top D + tI_m)^{-1} D^\top) < 1$.

Next we will derive the upper bound of eigenvalues of the above matrix. First, for any eigenvalue d and corresponding nonzero eigenvector u of $Z^\top Z = X_A J X_A$, we have

$$du^\top u = u^\top X_A^\top J X_A u = \begin{bmatrix} u \\ 0 \end{bmatrix}^\top X^\top J X \begin{bmatrix} u \\ 0 \end{bmatrix} \leq \lambda_{\max}(X^\top J X) u^\top u,$$

hence $d \leq \lambda_{\max}(X^\top J X)$. Then again, for any eigenvalue c and corresponding nonzero eigenvector v of $X^\top J X$, we have

$$cv^\top v = v^\top X^\top J X v = \sum_i J_{ii} v^\top x_i x_i^\top v \leq \sum_i v^\top x_i x_i^\top v = v^\top X^\top X v \leq \lambda_{\max}(X^\top X) v^\top v,$$

implying that $c \leq \lambda_{\max}(X^\top X)$.

Therefore, we have $d \leq \lambda_{\max}(X^\top JX) \leq \lambda_{\max}(X^\top X)$. Then since the eigenvalues of $Z^\top Z$ are the diagonal elements of D , the eigenvalues of $D(D^\top D + tI_m)^{-1}D^\top$ are bounded by $\frac{\lambda_{\max}(X^\top X)^2}{\lambda_{\max}(X^\top X)^2 + t}$.

Then recall $t = n\gamma\lambda(1 - \alpha)$ and $a^\top a \geq 1$, we have

$$\begin{aligned}
& \mathbf{1}_n^\top \Psi \mathbf{1}_n - \mathbf{1}_n^\top \Psi X_A (X_A^\top \Psi X_A + \lambda(1 - \alpha)I_{|A|})^{-1} X_A^\top \Psi \mathbf{1}_n \\
&= \frac{1}{n\gamma} (a^\top a - (U^\top a)^\top D(D^\top D + tI_m)^{-1} D^\top (U^\top a)) \\
&\geq \frac{1}{n\gamma} (a^\top a - \frac{\lambda_{\max}(X^\top X)^2}{\lambda_{\max}(X^\top X)^2 + t} (U^\top a)^\top U^\top a) \\
&= \frac{1}{n\gamma} \times \frac{n\gamma\lambda(1 - \alpha)}{\lambda_{\max}(X^\top X)^2 + n\gamma\lambda(1 - \alpha)} a^\top a \\
&\geq \frac{\lambda(1 - \alpha)}{\lambda_{\max}(X^\top X)^2 + n\gamma\lambda(1 - \alpha)} \\
&> 0
\end{aligned}$$

Let

$$H_{31} = \begin{bmatrix} \mathbf{1}_n^\top \Psi \mathbf{1}_n & \mathbf{1}_n^\top \Psi X_A \\ X_A^\top \Psi \mathbf{1}_n & X_A^\top \Psi X_A + \lambda(1 - \alpha)I_{|A|} \end{bmatrix}, \quad H_{32} = \begin{bmatrix} X_B^\top \Psi \mathbf{1}_n & X_B^\top \Psi X_A \end{bmatrix}, \quad H_{33} = \lambda\alpha I_{|B|}.$$

Observe that $H_{33}^{-1} = \frac{1}{\lambda\alpha} I_{|B|}$. Then if H_{31} is invertible, we have

$$H_3^{-1} = \begin{bmatrix} H_{31}^{-1} & \mathbf{0} \\ -\frac{1}{\lambda\alpha} H_{32} H_{31}^{-1} & \frac{1}{\lambda\alpha} I_{|B|} \end{bmatrix}.$$

Hence to show H_3 is invertible, it suffices to show H_{31} is invertible. Let

$$M = X_A^\top \Psi X_A + \lambda(1 - \alpha)I_{|A|}, \quad b = X_A^\top \Psi \mathbf{1}_n,$$

and

$$\kappa = \mathbf{1}_n^\top \Psi \mathbf{1}_n - \mathbf{1}_n^\top \Psi X_A (X_A^\top \Psi X_A + \lambda(1 - \alpha)I_{|A|})^{-1} X_A^\top \Psi \mathbf{1}_n.$$

Since $\kappa > 0$, we have

$$H_{31}^{-1} = \begin{bmatrix} \frac{1}{\kappa} & -\frac{1}{\kappa} b^\top M^{-1} \\ -\frac{1}{\kappa} M^{-1} b & M^{-1} + \frac{1}{\kappa} M^{-1} b b^\top M^{-1} \end{bmatrix},$$

and it follows that H_3 is invertible.

It can be easily shown that $\|b\| = \|b^\top\| \leq \frac{1}{\sqrt{n\gamma}} \|X\|$, $\|M^{-1}\| \leq \frac{1}{\lambda(1-\alpha)}$. Combine this with $\frac{1}{\kappa} \leq \frac{\lambda_{\max}(X^\top X)^2 + n\gamma\lambda(1-\alpha)}{\lambda(1-\alpha)}$, then similar to (A.3), we have

$$\|H_{31}^{-1}\| \leq \frac{1}{\lambda(1-\alpha)} + \frac{\lambda_{\max}(X^\top X)^2 + n\gamma\lambda(1-\alpha)}{\lambda(1-\alpha)} \left(1 + \frac{\|X\|}{\sqrt{n\gamma\lambda(1-\alpha)}}\right)^2$$

and then

$$\|H_3^{-1}\| \leq \frac{1}{\lambda\alpha} + \left[\frac{1}{\lambda(1-\alpha)} + \frac{\lambda_{\max}(X^\top X)^2 + n\gamma\lambda(1-\alpha)}{\lambda(1-\alpha)} \left(1 + \frac{\|X\|}{\sqrt{n}\gamma\lambda(1-\alpha)}\right)^2 \right] \left(1 + \frac{2\|X\|}{\sqrt{n}\gamma\lambda\alpha}\right).$$

Proof of Theorem 5.1.

Without loss of generality, assume θ_k has exactly one cluster point θ^* , i.e. $\theta_k \rightarrow \theta^*$.

Notice that

$$|t| - \frac{\gamma}{2} \leq h_\gamma(t) \leq |t|,$$

hence

$$f_A(\theta; \lambda) - \frac{\gamma}{2} \leq f_H(\theta; \lambda, \gamma) \leq f_A(\theta; \lambda).$$

Let $\hat{\theta}_A$ be a minimizer of $f_A(\theta; \lambda)$, and $f_A^0 = \min_{\theta} f_A(\theta; \lambda) = f_A(\hat{\theta}_A; \lambda)$, then

$$f_H(\theta_k; \lambda, \gamma_k) \leq f_H(\hat{\theta}_A; \lambda, \gamma_k) \leq f_A(\hat{\theta}_A; \lambda) = f_A^0.$$

For any $\epsilon > 0$, there exists K such that for $k \geq K$, $\gamma_k < 2\epsilon$, then

$$f_H(\theta_k; \lambda, \gamma_k) \geq f_A(\theta_k; \lambda) - \epsilon \geq f_A^0 - \epsilon.$$

Hence for $k \geq K$,

$$f_A^0 - \epsilon \leq f_A(\theta_k; \lambda) - \epsilon \leq f_A^0.$$

Let $k \rightarrow \infty$, we have $f_A^0 \leq f_A(\theta^*) \leq f_A^0 + \epsilon$. Since ϵ is arbitrary, $f_A(\theta^*) = f_A^0$.

Proof of Theorem 5.2.

Without loss of generality, assume θ_k has exactly one cluster point θ^* , i.e. $\theta_k \rightarrow \theta^*$.

Notice that

$$\gamma h_\gamma(t) \leq \frac{1}{2}t^2,$$

which implies

$$\gamma f_H(\theta; \lambda/\gamma, \gamma) \leq f_S(\theta; \lambda).$$

Let $\hat{\theta}_S$ be a minimizer of $f_S(\theta; \lambda)$, and $f_S^0 = \min_{\theta} f_S(\theta; \lambda) = f_S(\hat{\theta}_S; \lambda)$, then

$$\gamma_k f_H(\theta_k; \lambda/\gamma_k, \gamma_k) \leq \gamma_k f_H(\hat{\theta}_S; \lambda/\gamma_k, \gamma_k) \leq f_S(\hat{\theta}_S; \lambda) = f_S^0.$$

Since $\theta_k = (\beta_0^k, \beta^k)$ is convergent, $r^k = y - \beta_0^k 1 - X\beta^k$ is convergent too. Then there exists $M > 0$ such that $\|r^k\|_\infty \leq M$. There exists K such that for $k \geq K$, $\gamma_k > M$, then $h_\gamma(r_i k) = \frac{1}{2}r_i k^2$, and

$$\gamma_k f_H(\theta_k; \lambda/\gamma_k, \gamma_k) = f_S(\theta_k; \lambda).$$

Hence for $k \geq K$,

$$f_S(\theta_k; \lambda) \leq f_S^0.$$

Let $k \rightarrow \infty$, we have $f_S(\theta^*; \lambda) \leq f_S^0$. Since $f_S(\theta^*; \lambda) \geq \min_{\theta} f_S(\theta; \lambda) = f_S^0$, $f_S(\theta^*) = f_S^0$.

References

Barro, R. J. and Lee, J.-W. (1994). Data set for a panel of 138 countries. <http://www.nber.org/pub/barro.lee/>.

Breheny, P. and Huang, J. (2011). Coordinate descent algorithms for nonconvex penalized regression, with applications to biological feature selection. *The Annals of Applied Statistics*, 5(1):232–253.

Chen, X., Nashed, Z., and Qi, L. (2000). Smoothing methods and semismooth methods for nondifferentiable operator equations. *SIAM Journal on Numerical Analysis*, 38(4):1200–1216.

Combettes, P. L. and Wajs, V. R. (2005). Signal recovery by proximal forward-backward splitting. *Multiscale Modeling & Simulation*, 4(4):1168–1200.

Friedman, J., Hastie, T., Höfling, H., and Tibshirani, R. (2007). Pathwise coordinate optimization. *The Annals of Applied Statistics*, 1(2):302–332.

Friedman, J., Hastie, T., and Tibshirani, R. (2010). Regularization paths for generalized linear models via coordinate descent. *Journal of Statistical Software*, 33(1):1–22.

Holland, P. W. and Welsch, R. E. (1977). Robust regression using iteratively reweighted least-squares. *Communications in Statistics-Theory and Methods*, 6(9):813–827.

Huber, P. J. (1973). Robust regression: asymptotics, conjectures and monte carlo. *The Annals of Statistics*, 1(5):799–821.

Huber, P. J. (1981). *Robust Statistics*. New York: John Wiley.

Ito, K. and Kunisch, K. (2008). *Lagrange Multiplier Approach to Variational Problems and Applications*. Philadelphia, PA: SIAM.

Koenker, R. (2005). *Quantile Regression*. New York: Cambridge University Press.

Koenker, R. and Bassett Jr, G. (1978). Regression quantiles. *Econometrica*, 46(1):33–50.

Koenker, R. and Machado, J. A. (1999). Goodness of fit and related inference processes for quantile regression. *Journal of the American Statistical Association*, 94(448):1296–1310.

Mifflin, R. (1977). Semismooth and semiconvex functions in constrained optimization. *SIAM Journal on Control and Optimization*, 15(6):959–972.

Qi, L. (1993). Convergence analysis of some algorithms for solving nonsmooth equations. *Mathematics of Operations Research*, 18(1):227–244.

Qi, L. and Sun, J. (1993). A nonsmooth version of newton’s method. *Mathematical Programming*, 58(1–3):353–367.

Rockafellar, R. T. (1970). *Convex Analysis*. Princeton, NJ: Princeton University Press.

Simon, N., Friedman, J., Hastie, T., and Tibshirani, R. (2011). Regularization paths for cox’s proportional hazards model via coordinate descent. *Journal of Statistical Software*, 39(5):1–13.

Tibshirani, R. (1996). Regression shrinkage and selection via the lasso. *Journal of the Royal Statistical Society. Series B (Methodological)*, 58(1):267–288.

Tibshirani, R., Bien, J., Friedman, J., Hastie, T., Simon, N., Taylor, J., and Tibshirani, R. J. (2012). Strong rules for discarding predictors in lasso-type problems. *Journal of the Royal Statistical Society: Series B (Statistical Methodology)*, 74(2):245–266.

Tseng, P. (2001). Convergence of a block coordinate descent method for nondifferentiable minimization. *Journal of Optimization Theory and Applications*, 109(3):475–494.

Wu, T. T. and Lange, K. (2008). Coordinate descent algorithms for lasso penalized regression. *The Annals of Applied Statistics*, 2(1):224–244.

Zou, H. and Hastie, T. (2005). Regularization and variable selection via the elastic net. *Journal of the Royal Statistical Society: Series B (Statistical Methodology)*, 67(2):301–320.